Inorg. Chem. **2003**, *42*, 4190–4203

Stability and Three-Dimensional Aromaticity of *closo*-$NB_{n-1}H_n$ Azaboranes, $n = 5$–12

Katayoun Najafian,[†] Paul von Rague Schleyer,*[,‡] and Thomas T. Tidwell[†]

Departments of Chemistry, University of Toronto, Toronto, Ontario, Canada M5S 3H6, and University of Georgia, Athens, Georgia 30602

Received January 24, 2003

Computations on all the possible positional isomers of the *closo*-azaboranes $NB_{n-1}H_n$ ($n = 5$–12) reveal substantial differences in the relative energies. Data at the B3LYP/6-311+G** level of density functional theory (DFT) agree well with expectations based on the topological charge stabilization, with the qualitative connectivity preferences of Williams, and with the Jemmis–Schleyer six interstitial electron rules. The energetic relationship involving each of the most stable positional isomers, 1-NB_4H_5, NB_5H_6, 2-NB_6H_7, 1-NB_7H_8, 4-NB_8H_9, 1-NB_9H_{10}, 2-$NB_{10}H_{11}$, $NB_{11}H_{12}$, was based on the energies (ΔH) of the model reaction: $NBH_2 + (n-1)BH_{increment} \rightarrow NB_nH_{n+1}$ ($n = 4$–11). This evaluation shows that the stabilities of *closo*-azaboranes $NB_{n-1}H_n$ ($n = 5$–12) increase with increasing cluster size from 5 to 12 vertexes. The "three-dimensional aromaticity" of these *closo*-azaboranes $NB_{n-1}H_n$ ($n = 5$–12) is demonstrated by their the nucleus-independent chemical shifts (NICS) and their magnetic susceptibilities (χ), which match one another well. However, there is no direct relationship between these magnetic properties and the relative stabilities of the positional isomers of each cluster. As expected, other energy contributions such as topological charge stabilization and connectivity can be equally important.

Introduction

The chemistry of boron is dominated by its electron deficient character resulting in three-dimensional delocalized electronic structures.[1−7,10a] The unusual deltahedral bonding, high stability, and aromaticity of *closo*-borane dianions, $B_nH_n^{2-}$ ($n = 5-12$), are now well understood.[1−7] The three-dimensional delocalization in *closo*-boranes with *n* vertexes and including ($n + 1$) skeletal electron pairs was discussed by King and Rouvray.[7] Aihara evaluated the resonance energies associated with the "three-dimensional aromaticity" of *closo*-borane dianions. In agreement with its high stability, the most highly symmetrical $B_{12}H_{12}^{2-}$ (I_h) had the largest resonance stabilization (1.763β). In contrast, Aihara classified the $B_5H_5^{2-}$ (resonance energy 0.0β) as "nonaromatic".[8] However, our recent ab initio studies[9,10] showed $B_5H_5^{2-}$ to be stabilized by about 35 kcal/mol due to three-dimensional delocalization. Moreover, the isoelectronic 1,5-$C_2B_3H_5$ was shown to exhibit nonclassical, delocalized bonding.[11]

* Author to whom correspondence should be addressed. E-mail: schleyer@chem.uga.edu.
[†] University of Toronto.
[‡] University of Georgia.

(1) (a) Olah, G. A.; Wade, K.; Williams, R. E. *Electron Deficient Boron and Carbon Clusters*; John Wiley and Sons: New York, 1991. (b) Olah, G. A.; Surya Prakash, G. K.; Williams, R. E.; Field, L. D.; Wade, K. *Hypercarbon Chemistry*; Wiley: New York, 1987. (c) Wade, K. *Electron Deficient Compounds*; Nelson: London, 1971.
(2) (a) Mingos, D. M. P.; Wales, D. J. *Introduction to Cluster Chemistry*; Prentice Hall: Englewood Cliffs, NJ, 1990. (b) Minkin, V. I.; Minyaev, R. M.; Zhdanov, Yu. A. *Nonclassical Structures of Organic Compounds*; Mir Publishers: Moscow, 1987.
(3) (a) King, R. B. *Chem. Rev.* **2001**, *101*, 1119. (b) McKee, M. L.; Wang, Z.-X.; Schleyer, P. v. R. *J. Am. Chem. Soc.* **2000**, *122*, 4781. (c) Schleyer, P. v. R.; Najafian, K.; Mebel, A. M. *Inorg. Chem.* **1998**, *37*, 6765.
(4) (a) Muetterties, E. L. *Boron Hydride Chmesitry*; Academic Press: New York, 1975. (b) Onak, T. *Organoborane Chemistry*; Academic Press: New York, 1975. (c) Lipscomb, W. N. *Boron Hydrides*; W. A. Benjamin: New York, 1963.
(5) (a) Casanova, J. *The Borane, Carborane, Carbocation Continuum*; Wiley: New York, 1998. (b) Onak, T. In *Comprehensive Organometallic Chemistry II*; Abel, E. W., Stone, F. G., Wilkinson, G., Eds.; Elsevier Science Ltd.: Oxford, U.K., 1995; Vol. 1, Chapter 6.
(6) (a) Williams, R. E. In *Advances in Organometallic Chemistry*; Stone, F. G. A., West, R., Eds.; Academic Press: New York, 1994. (b) Liebman, J. F.; Greenberg A.; Williams, R. E. *Advances in Boron and the Boranes*; VCH Verlagsgesellschaft: New York, 1988.
(7) King, R. B.; Rouvray, D. H. *J. Am. Chem. Soc.* **1977**, *99*, 7834.
(8) Aihara, J. *J. Am. Chem. Soc.* **1978**, *100*, 3339.
(9) (a) Schleyer, P. v. R.; Subramanian, G.; Jiao, H.; Najafian, K.; Hofmann, M. In *Advances in Boron Chemistry*; Sibert, W., Ed.; The Royal Society of Chemistry: Cambridge, England, 1997. (b) Schleyer, P. v. R.; Subramanian, G.; Dransfeld, A. *J. Am. Chem. Soc.* **1996**, *118*, 9988.
(10) (a) Schleyer, P. v. R.; Najafian, K. In *The Borane, Carborane, Carbocation Continuum*; Casanova, J., Ed.; Wiley: New York, 1998. (b) Choi, C. H.; Kertesz, M. *J. Chem. Phys.* **1998**, *108*, 6681. (c) Wannere, C. S.; Schleyer, P. v. R. *Org. Lett.*, submitted.

10.1021/ic0340783 CCC: $25.00
Published on Web 06/05/2003

Recently *closo*-boranes with only one heteroatom,[12] e.g., $B_{11}H_{11}PR$,[13] $B_{11}H_{11}S$,[14] B_9H_9S,[15] $CB_{11}H_{12}^-$,[16,17] $CB_9H_{10}^-$,[18] $CB_{10}H_{11}^-$,[19] and $CB_7H_8^-$,[20] have been synthesized, but smaller monosubstituted *closo*-boranes remain unknown. Apparently, the incorporation of nitrogen as a heterovertex in polyhedral borane cages is more difficult synthetically than that in their isoelectronic relatives including the *closo*-dicarboranes, $C_2B_{n-2}H_n$ ($n = 5-12$),[21,22] and *closo*-monocarbaboranes, $CB_{n-1}H_n^-$ ($n = 5-12$).[23,24] Indeed, only two *closo*-azaboranes are known, NB_9H_{10}[25] and $NB_{11}H_{12}$.[26,27] We are not aware of any systematic theoretical studies in the literature. One of the goals of the present study is to evaluate the stabilities of *closo*-azaborane cages $NB_{n-1}H_n$ ($n = 5-12$) employing density functional theory.

Except for $n = 6$ and 12, perturbation of the cage by a single heteroatom leads to at least two possible positional isomers for a given cluster nuclearity. Three qualitative considerations can be used to predict the relative stabilities of the positional isomers in polyhedral *closo*-borane derivatives.

The first, due to Williams,[28] suggests that more electronegative atoms such as carbon or nitrogen usually prefer the least connected vertexes in order to minimize electron sharing. This empirical rule helps rationalize the positional isomer preferences of the neutral *closo*-dicarboranes, $C_2B_{n-2}H_n$ ($n = 5-12$),[29,30] and the *closo*-monocarbaborane anions, $CB_{n-1}H_n^-$ ($n = 5-12$),[30] and should be applicable to the *closo*-azaborane $NB_{n-1}H_n$ ($n = 5-12$) clusters as well.

Gimarc's topological charge stabilization rule[29] suggests that a more electronegative heteroatom should prefer sites of maximum electron density. This rule agrees well with the experimentally observed positional isomer preferences of the *closo*-dicarboranes and the *closo*-monocarbaborane anions.

Jemmis and Schleyer[31] extended the planar ($4n + 2$) Hückel rule to the aromaticity of three-dimensional delocalized systems using the "six interstitial electron" concept. They pointed to the need of orbital overlap compatibility. The radial extension of the π-orbitals of the capping atom should be matched optimally with the rings of the best size.

Recently,[30] our comprehensive RMP2(fc)/6-31G* ab initio computations on the *closo*-monocarbaboranes, $CB_{n-1}H_n^-$ ($n = 5-12$), and the *closo*-dicarboranes, $C_2B_{n-2}H_n$ ($n = 5-12$), found that the relative energies of all the positional isomers agree with the qualitative connectivity considerations of Williams,[28] with Gimarc's topological charge stabilization rule,[29] and with the available experimental data. In contrast to polybenzenoid hydrocarbons and [*n*]annulenes,[10] the stabilities of the *closo*-borane dianions, $B_nH_n^{2-}$ ($n = 5-12$), the *closo*-monocarbaborane anions, $CB_{n-1}H_n^-$ ($n = 5-12$), and the *closo*-dicarboranes, $C_2B_{n-2}H_n$ ($n = 5-12$), actually *increased* with increasing cluster size from 5 to 12 vertexes. These clusters exhibited magnetic behavior characteristic of "three-dimensional aromaticity".[30] The large nucleus-independent chemical shifts (NICS),[32-35] which are based on the negative of the absolute chemical shielding, computed at the cage centers, provide a direct measure of the ring current effects.[10] The most symmetric 12 and 6 vertex species have the largest NICS values, followed by those with 10 vertexes. The computed magnetic susceptibility data correspond well with NICS.[30] However, the aromaticity ordering based on these magnetic properties does not always agree with the relative stabilities of positional isomers of the same cluster, as in other cases[34,35] where connectivity and topological charge stabilization are important.

Since the *closo*-azaboranes $NB_{n-1}H_n$ ($n = 5-12$) have not been evaluated comprehensively before, one of our goals is

(11) Hofmann, M.; Fox, M. A.; Greatrex, R.; Schleyer, P. v. R.; Bausch, J. W.; Williams, R. E. *Inorg. Chem.* **1996**, *35*, 6170.
(12) Vondrak, T.; Hermanek, S.; Plesek, J. *Polyhedron* **1993**, *12*, 1301.
(13) (a) Little, J. C.; Moran, J. T.; Todd, L. J. *J. Am. Chem. Soc.* **1967**, *89*, 5495. (b) Getman, T. D.; Deng, H.-B.; Hsu, L.-Y.; Shore, S. G. *Inorg. Chem.* **1989**, *28*, 3612.
(14) Hynk, D.; Vajda, E.; Buhl, M.; Schleyer, P. v. R. *Inorg. Chem.* **1992**, *31*, 2464 and references therein.
(15) Pretzer, W. R.; Rudlph, R. W. *J. Am. Chem. Soc.* **1973**, *95*, 931.
(16) (a) Ivanov, S. V.; Lupinetti, A. J.; Miller, S. M.; Anderson, O. P.; Solntsev, K. A.; Strauss, S. H. *Inorg. Chem.* **1995**, *34*, 6419. (b) Knoth, W. H. Little, J. L.; Lawrence, J. R.; Scholer, F. R.; Todd, L. J. *Inorg. Synth.* **1968**, *11*, 33. (c) Knoth, W. H. *J. Am. Chem. Soc.* **1967**, *89*, 1274.
(17) (a) Srivastava, R. R.; Hamlin, D. K.; Wilbur, D. S. *J. Org. Chem.* **1996**, *61*, 9041. (b) Jelink, T.; Plesek, J.; Hermanek, S.; Stibr, B. *Collect. Czech. Chem. Commun.* **1986**, *51*, 819. (c) Jelink, T.; Baldwin, P.; Scheidt, W. R.; Reed, C. A. *Inorg. Chem.* **1982**, *1003*, 32.
(18) (a) Ivanov, S. V.; Rockwell, J. J.; Miller, S. M.; Anderson, O. P.; Solntsev, K. A.; Strauss, S. H. *Inorg. Chem.* **1996**, *35*, 7882. (b) Xie, Z.; Liston, D. J.; Jelnik, T.; Mitro, V.; Bau, R.; reed, C. A. *J. Chem. Soc., Chem. Commun.* **1993**, 384.
(19) Wiersema, R. J.; Hawthorne, M. F. *Inorg. Chem.* **1973**, *12*, 785.
(20) (a) Jelinek, T.; Stibr, B.; Plesek, J.; Kennedy, J. D.; Thornton-Pett, M. *J. Chem. Soc., Dalton Trans.* **1995**, 431. (b) Plesek, J.; Jelinek, T.; Stibr, B.; Hermanek, S. *J. Chem. Soc., Chem. Commun.* **1988**, 384.
(21) For example: (a) Gimarc, B. M.; Zaho, M. *Inorg. Chem.* **1996**, *35*, 825. (b) Bregadze, V. I. *Chem. Rev.* **1992**, *92*, 209 and references therein. (c) Plesek, J. *Chem. Rev.* **1992**, *92*, 269 and references therein. (d) Gimarc, B. M.; Dai, B.; Ott, J. *J. Comput. Chem.* **1989**, *10*, 14.
(22) For example: (a) Hynk, D.; Rankin, D. W. H.; Roberston, H. E.; Hofmann, M.; Schleyer, P. v. R.; Buhl, M. *Inorg. Chem.* **1994**, *33*, 4781. (b) Schleyer, P. v. R.; Gauss, J.; Buhl, M.; Greatrex, R. A.; Fox, M. A. *J. Chem. Soc., Chem. Commun.* **1993**, *23*, 1766. (c) Buhl, M.; Mebel, A. M.; Charkin, O.; Schleyer, P. v. R. *Inorg. Chem.* **1992**, *31*, 3769. (d) Buhl, M.; Schleyer, P. v. R. *J. Am. Chem. Soc.* **1992**, *114*, 477. (e) Buhl, M.; Gauss, J.; Hofmann, M.; Schleyer, P. v. R. *Inorg. Chem.* **1992**, *31*, 3769.
(23) For example: (a) Xie, Z.; Jelinek, T.; Bau, R.; Reed, C. A. *J. Am. Chem. Soc.* **1994**, *116*, 1907. (b) Xie, Z.; Bau, R.; Reed, C. A. *Angew. Chem., Int. Ed. Engl.* **1994**, *33*, 2433. (c) Reed, C. A.; Xie, Z.; Bau, R.; Benesi, A. *Science* **1993**, *262*, 402.
(24) For example: (a) Ivanov, S. V.; Rockwell, J. J.; Miller, S. M.; Anderson, O. P.; Solnstev, K. A.; Strauss, S. H. *Inorg. Chem.* **1996**, *35*, 7882. (b) Nestor, K.; Stibr, B.; Kennedy, J. D.; Thornton-Pett, M.; Jelinek, T. *Collect. Czech. Chem. Commun.* **1992**, *57*, 1262.
(25) Arafat, A.; Baer, J.; Huffman, J. C.; Todd, L. J. *Inorg. Chem.* **1986**, *25*, 3757.
(26) Muller, J.; Runsik, J.; Paetzold, P. *Angew. Chem., Int. Ed. Engl.* **1991**, *30*, 175.
(27) Hynk, D.; Buhl, M.; Schleyer, P. v. R.; Volden, H. V.; Gunderson, S.; Muller, J.; Paetzold, P. *Inorg. Chem.* **1993**, *32*, 2442.
(28) Williams, R. E. *Adv. Inorg. Chem. Radiochem.* **1976**, *18*, 67.
(29) Ott, J. J.; Gimarc, B. M. *J. Am. Chem. Soc.* **1986**, *108*, 4303.
(30) Schleyer, P. v. R.; Najafian, K. *Inorg. Chem.* **1998**, *37*, 3454.
(31) (a) Jemmis, E. D. *J. Am. Chem. Soc.* **1982**, *104*, 7017. (b) Jemmis, E. D.; Schleyer, P. v. R. *J. Am. Chem. Soc.* **1982**, *104*, 4781.
(32) Schleyer, P. v. R.; Jiao, H. *Pure Appl. Chem.* **1996**, *68*, 209.
(33) (a) Schleyer, P. v. R.; Jiao, H.; Hommes, N. J. R. v. E. *J. Am. Chem. Soc.* **1997**, *119*, 12669. (b) Jiao, H.; Schleyer, P. v. R. *Angew. Chem., Int. Ed. Engl.* **1996**, *35*, 2383. (c) Subramanian, G.; Schleyer, P. v. R.; Jiao, H. *Angew. Chem., Int. Ed. Engl.* **1996**, *35*, 2638.
(34) (a) Subramanian, G.; Schleyer, P. v. R.; Jiao, H. *Organometallics* **1997**, *16*, 2362. (b) Novak, I. *J. Mol. Struct. (THEOCHEM)* **1997**, *398*, 315.
(35) Subramanian, G.; Schleyer, P. v. R.; Jiao, H. *Angew. Chem., Int. Ed. Engl.* **1996**, *35*, 2638.

Table 1. Data for *closo*-Borane Dianions, $B_nH_n^{2-}$ ($n = 5-12$): Total Energies (au), Zero Point Energies (ZPE, kcal/mol),[a] Reaction Energies from Eq 1 (ΔH),[b] and Magnetic Susceptibilities (χ, ppm cgs)[c]

molecule	sym	ZPE[a]	B3LYP/6-311+G**	ΔH[b]	χ[c]
$B_5H_5^{2-}$	D_{3h}	36.68	−127.17130	−156.99	−75.09
$B_6H_6^{2-}$	O_h	47.12	−152.72452	−242.75	−85.10
$B_7H_7^{2-}$	D_{5h}	56.30	−178.21180	−288.40	−87.81
$B_8H_8^{2-}$	D_{2d}	65.06	−203.68894	−328.10	−96.17
$B_9H_9^{2-}$	D_{3h}	74.45	−229.19051	−382.51	−119.32
$B_{10}H_{10}^{2-}$	D_{4d}	84.71	−254.71361	−449.56	−144.26
$B_{11}H_{11}^{2-}$	C_{2v}	93.22	−280.18060	−483.14	−148.20
$B_{12}H_{12}^{2-}$	I_h	104.77	−305.76290	−586.06	−162.71
$B_2H_2^{2-}$	$D_{\infty h}$	10.43	−50.67952		−46.13
B_3H_5	C_{2v}	32.09	−77.44676		+0.34
B_2H_4	D_{2h}	24.56	−52.03472		−1.85

[a] Zero point energies (ZPE, kcal/mol), calculated at B3LYP/6-31G*. [b] $B_2H_2^{2-} + (n-2)BH_{increment} \rightarrow B_nH_n^{2-}$ ($n = 5-12$) (eq 1) at B3LYP/6-311+G**, with ZPE correction (ref 39) scaled by 0.98 in kcal/mol. Note that $B_2H_2^{2-}$ ($D_{\infty h}$) data were used and that the BH_{inc} increment was taken as the difference in energy between B_3H_5 (C_{2v}, planar form) and B_2H_4 (D_{2h}, ethylene like) since inherent stabilization due to hyperconjugation or to delocalization is absent. [c] Magnetic susceptibility at CSGT-B3LYP/6-311+G**//B3LYP/6-311+G**.

Table 2. Data for *closo*-Monocarbaborane Anions, $CB_{n-1}H_n^-$ ($n = 5-12$): Total Energies (au), Zero Point Energies (ZPE, kcal/mol),[a] and Relative Energies[b]

molecule	sym	ZPE[a]	B3LYP/6-311+G**	rel energy[b]
$CB_4H_5^-$				
1	C_{3v}	41.33 (0)	−140.58607	0.00
2	C_{2v}	40.06 (0)	−140.54692	23.31
$CB_5H_6^-$				
3	C_{4v}	51.43 (0)	−166.101098	0.00
$CB_6H_7^-$				
4	C_{2v}	60.55 (0)	−191.58384	0.00
5	C_{5v}	59.69 (0)	−191.53629	30.00
$CB_7H_8^-$				
6	C_s	69.33 (0)	−217.04979	0.00
7	C_s	68.27 (1)	−217.01290	22.10
8	C_{3v}	65.21 (0)	−216.96237	50.79
9	C_s	65.79 (0)	−216.91038	83.96
$CB_8H_9^-$				
10	C_{2v}	78.70 (0)	−242.54224	0.00
11	C_s	77.86 (0)	−242.50989	19.46
$CB_9H_{10}^-$				
12	C_{4v}	88.98 (0)	−268.05625	0.00
13	C_s	88.34 (0)	−268.02326	20.06
$CB_{10}H_{11}^-$				
14	C_s	97.41 (0)	−293.51193	0.00
15	C_s	97.00 (0)	−293.48226	18.20
16	C_s	96.84 (0)	−293.47934	19.88
17	C_2	96.10 (1)	−293.46061	30.90
$CB_{11}H_{12}^-$				
18	C_{5v}	108.81 (0)	−319.05723	0.00
CBH_2^-	$C_{\infty v}$		64.11691	

[a] Zero point energy (kcal/mol), calculated at B3LYP/6-31G(d). In parentheses, number of imaginary frequencies NIMAG. [b] The relative energies with ZPE corrections scaled by 0.98 (ref 39) in kcal/mol.

to use computed DFT data to test the relative stability predictions based on the qualitative considerations described above. Comparison of the *closo*-borane dianions $B_nH_n^{2-}$ with the isoelectronic *closo*-azaboranes $NB_{n-1}H_n$ reveals the effects of the electronegative nitrogen atom substitution. We also assess the "three-dimensional aromaticity" of these clusters by applying magnetic criteria, e.g., NICS[36] and magnetic susceptibility exaltation, Λ.[31] The results are compared with those obtained for the *closo*-borane dianions $B_nH_n^{2-}$ and *closo*-monocarbaborane anions, $CB_{n-1}H_n^-$ ($n = 5-12$).[30]

Table 3. Data for *closo*-Azaboranes, $NB_{n-1}H_n$ ($n = 5-12$): Total Energies (au), Zero Point Energies (ZPE, kcal/mol),[a] and Relative Energies[b]

molecule	sym	ZPE[a]	B3LYP/6-311+G**	rel energy[b]
NB_4H_5				
19	C_{3v}	43.24 (0)	−157.22270	0.00
20	C_2	42.00 (0)	−157.19816	14.18
20	C_s	40.51 (1)	−157.14145	48.28
20	C_{2v}	40.28 (2)	−157.14133	48.13
NB_5H_6				
21	C_{4v}	52.50 (0)	−182.69360	0.00
NB_6H_7				
22	C_s	61.29 (0)	−208.17426	0.00
23	C_{5v}	59.55 (0)	−208.09221	49.75
NB_7H_8				
24	C_s	70.13 (0)	−233.62703	0.00
25	C_{3v}	67.76 (0)	−233.59797	15.90
26	C_s	69.11 (1)	−233.59257	20.61
NB_8H_9				
27	C_s	79.70 (0)	−259.10899	0.00
27	C_{2v}	79.46 (1)	−259.10862	0.00
28	C_s	78.68 (0)	−259.08411	14.60
NB_9H_{10}				
29	C_{4v}	89.98 (0)	−284.61614	0.00
30	C_s	87.99 (0)	−284.56041	33.00
$NB_{10}H_{11}$				
31	C_s	98.09 (0)	−310.06449	0.00
32	C_s	96.74 (0)	−310.01037	32.61
33	C_s	96.53 (0)	−310.00388	36.48
34	C_s	94.89 (2)	−309.99504	40.42
$NB_{11}H_{12}$				
35	C_{5v}	108.76 (0)	−335.57682	0.00
NBH_2	$C_{\infty v}$	15.89 (0)	−80.83477	

[a] Zero point energy (kcal/mol), calculated at B3LYP/6-31G(d). In parentheses, number of imaginary frequencies NIMAG. [b] The relative energies with ZPE corrections scaled by 0.98 (ref 39) in kcal/mol.

Computational Methods

The geometries of *closo*-borane dianions $B_nH_n^{2-}$ ($n = 5-12$), *closo*-monocarbaborane anions $CB_{n-1}H_n^-$ ($n = 5-12$), and *closo*-azaboranes $NB_{n-1}H_n$ ($n = 5-12$) were optimized within chosen symmetry restrictions using the GAUSSIAN 98[38] program first at the B3LYP/6-31G* level of density functional theory. Vibration frequency calculations at B3LYP/6-31G* characterized the stationary points and provide the zero-point energy (ZPE) corrections.[39] Minima had no imaginary frequencies, and transition states had one imaginary frequency. The geometry and energy data in Tables 1−3 are optimized at B3LYP/6-311+G**. Natural population

(36) Schleyer, P. v. R.; Maerker, C.; Dransfeld, A.; Jiao, H.; Hommes, N. J. R. v. E. *J. Am. Chem. Soc*. **1996**, *118*, 6317.

(37) (a) Dauben, H. P., Jr.; Wilson, J. D.; Laity, J. L. J. In *Nonbenzenoid Aromatics*; Snyder, J. P., Ed.; Academic Press: New York, 1971; Vol. 2, pp 167−206. (b) Dauben, H. P., Jr.; Wilson, J. D.; Laity, J. L. *J. Am. Chem. Soc*. **1969**, *91*, 1991. (c) Dauben, H. P., Jr.; Wilson, J. D.; Laity, J. L. *J. Am. Chem. Soc*. **1968**, *90*, 811.

(38) Frisch, M. J.; Trucks, G. W.; Schlegel, H. B.; Scuseria, G. E.; Robb, M. A.; Cheeseman, J. R.; Zakrzewski, V. G.; Montgomery, J. A., Jr.; Stratmann, R. E.; Burant, J. C.; Dapprich, S.; Millam, J. M.; Daniels, A. D.; Kudin, K. N.; Strain, M. C.; Faraks, O.; Tomasi, J.; Barone, V.; Cossi, M.; Cammi, R.; Mennucci, B.; Pomelli, C.; Adamo, C.; Clifford, S.; Ochterski, J.; Petersson, G. A.; Ayala, P. Y.; Cui, Q.; Morokuma, K.; Malick, D. K.; Rabuck, A. D.; Raghavachari, K.; Foresman, J. B.; Cioslowski, J.; Oritz, J. V.; Stefanov, B. B.; Liu, G.; Liashenko, A.; Piskorz, P.; Komaromi, I.; Gomperts, R.; Martin, R. L.; Fox, D. J.; Keith, T.; Al-Laham, M. A.; Peng, C. Y.; Nanayakkara, A.; Gonzalez, C.; Challacombe, M.; Gill, P. M. W.; Johnson, B.; Chen, W.; Wong, M. W.; Andres, J. L.; Head-Gordon, M.; Replogle, E. S.; Pople, J. A. *Gaussian 98*; Gaussian, Inc.: Pittsburgh, PA, 1998. (b) See: *The Encyclopedia of Computational Chemistry*; Schleyer, P. v. R., Allinger, N. L., Clark, T., Gasteiger, J., Kollman, P. A., Schaefer, H. F., III, Schreiner, P. R., Eds.; John Wiley & Sons: Chichester, 1998.

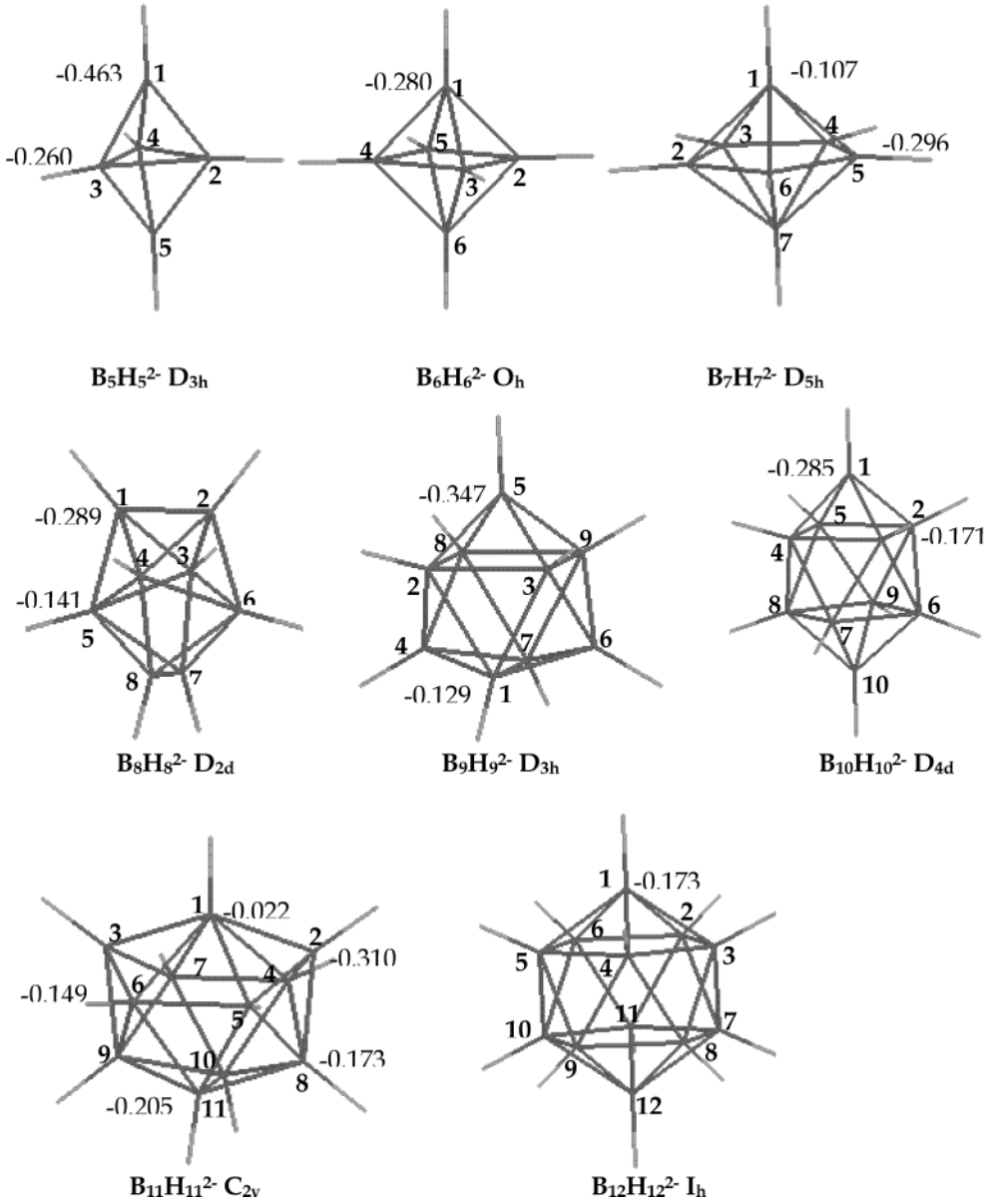

Figure 1. Natural charges obtained at B3LYP/6-311+G** level for *closo*-borane dianions, $B_nH_n^{2-}$ ($n = 5-12$).

analysis (NPA)[40] obtained at the same level for the *closo*-borane dianions $B_nH_n^{2-}$ ($n = 5-12$) are included in Figure 1. Relative reaction energies ΔH are given for *closo*-borane dianions $B_nH_n^{2-}$ ($n = 5-12$) in Table 1, *closo*-monocarbaborane anions $CB_{n-1}H_n^-$ ($n = 5-12$) in Table 2, and *closo*-azaboranes $NB_{n-1}H_n$ ($n = 5-12$) in Table 3 and include zero point energies scaled by a factor of 0.98. The NICS and magnetic susceptibilities were computed at CSGT-B3LYP/6-311+G**,[41] using the B3LYP/6-311+G** optimized geometries.

Results and Discussion

Ring−Cap Orbital Overlap Match: Interaction of the B_nH_n Ring with the Caps (X = BH, CH, NH). The relative stabilities of the isoelectronic *closo*-XYB_nH_n ($n = 3-5$; X, Y = NH, CH, BH) can be understood by considering the ring−cap orbital overlap match.[31] These cages are pictured as arising from the interaction of a B_nH_n ring with capping groups (X, Y) on both sides, leading to bipyramidal structures. The degree of cap−ring interaction depends on the radial extension (diffuseness) of the p-orbital of the cap, the ring size, and the ring−cap distance.[31] The most stable form is found when the ring−cap orbital interaction benefits from the maximum possible overlap, that is, the best "fit."

The out-of-plane bending of the ring hydrogens indicates the degree of orbital compatibility.[31] Scheme 1 illustrates general cases. The orbitals of the B_nH_n ring and the capping groups (X and Y, shown to be the same in Scheme 1a and Scheme 1b) overlap ineffectively. In contrast, Scheme 1c shows an ideal ring−cap interaction with maximal overlap. In *closo*-XYB_nH_n ($n = 3-5$; where X = NH or CH and Y

(39) Scott, A. P.; Radom, L. *J. Phys. Chem.* **1996**, *100*, 16502 and references therein.
(40) (a) Reed, A. E.; Schleyer, P. v. R. J. *Am. Chem. Soc.* **1990**, *112*, 1434. (b) Reed, A. E.; Weinhold, F. *Chem. Rev.* **1988**, *88*, 899.
(41) (a) Bader, R. F.; Keith, T. A. *J. Chem. Phys.* **1993**, *99*, 3683. (b) Keith, T. A.; Bader, R. F. W. *Chem. Phys. Lett.* **1992**, *194*, 1.

Scheme 1

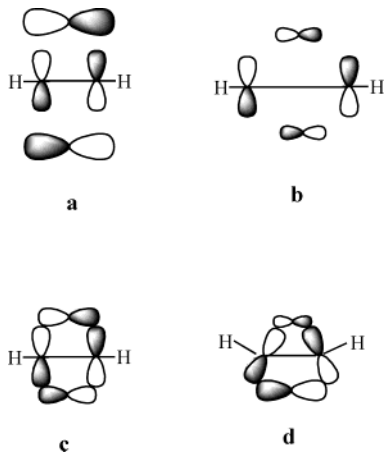

Table 4. Selected Bond Lengths (Å), Bond Angles (deg), and Wiberg Bond Indexes (WBI) of *closo*-Heteroboranes, XYB_nH_n ($n = 3-5$, X, Y = NH, CH, BH), Obtained at the B3LYP/6-311+G** Level

		θ^c			$B_{center}-Y$		
X[a]	Y[b]	B_3H_3	B_4H_4	B_5H_5	B_3H_3	B_4H_4	B_5H_5
BH^-	BH^-	0.00	0.00	0.00	1.307	1.228	1.168
BH	CH	4.53	7.71	8.96	1.140	1.081	1.040
BH	NH	8.19	14.53	15.91	1.110	1.044	1.053

		B_c-X			B−X		
X[a]	Y[b]	B_3H_3	B_4H_4	B_5H_5	B_3H_3	B_4H_4	B_5H_5
BH^-	BH^-	1.307	1.228	1.168	1.680	1.737	1.830
BH	CH	1.285	1.227	1.181	1.666	1.728	1.827
BH	NH	1.225	1.201	1.131	1.655	1.714	1.807

		B−B					
		D			WBI		
X[a]	Y[b]	B_3H_3	B_4H_4	B_5H_5	B_3H_3	B_4H_4	B_5H_5
BH^-	BH^-	1.827	1.737	1.657	0.462	0.683	0.836
BH	CH	1.832	1.720	1.639	0.373	0.600	0.750
BH	NH	1.851	1.730	1.657	0.369	0.572	0.712

		B−Y		
X[a]	Y[b]	B_3H_3	B_4H_4	B_5H_5
BH^-	BH^-	1.680	1.737	1.830
BH	CH	1.555	1.627	1.740
BH	NH	1.513	1.608	1.759

[a] X = capping group with more diffuse orbital. [b] Y = capping group with less diffuse orbital. [c] θ = out-of-plane bending of the external B−H bonds of the B_nH_n, $n = 3-5$, ring toward Y.

= BH), the hydrogens bend (θ deg) toward the heteroatom apex with its less diffuse orbitals. This bending rehybridizes the π-orbitals of the ring and increases their interaction with the cap. However, the rehybridized π-orbitals of the ring bend away from the cap on the other side (Scheme 1d), and this may be unfavorable unless the second cap has more diffuse orbitals.

The concept of the compatibility of orbitals with regard to their overlap[31] helps explain the geometries and predicts the best X, Y combinations for capping a specific B_nH_n ring. Thus, in monoheteroatom substituted cages, XYB_3H_3 (Y = CH or NH, X = BH), the out-of-plane bending is smaller (4.53°) when Y = CH than when Y = NH (8.19°, Table 4) since the latter has less diffuse orbitals. The ring center to cap distance, $B_{center}-Y$ (B_{center} is the center of the borocycle ring), also shortens as the effective size of the cap orbitals decreases. Thus, the $B_{center}-Y$ distance decreases in going from $B_5H_5^{2-}$ (1.307 Å) to 1-$CB_4H_5^-$ (**1**) (1.140 Å) to 1-NB_4H_5 (**19**) (1.110 Å). 1-NB_4H_5 has the smallest ring center to cap distance and the largest out-of-plane bending (θ) toward the cap (Table 4).

Table 5. Selected Bond Lengths (Å), Bond Angles (deg), and Wiberg Bond Indexes (WBI) of *closo*-Heteroboranes, XYB_nH_n ($n = 3-5$, X, Y = NH, CH, BH for 8, 10, and 12 Vertexes), Obtained at the B3LYP/6-311+G** Level

		θ^c			$B_{center}-Y$		
X[a]	Y[b]	B_3H_3	B_4H_4	B_5H_5	B_3H_3	B_4H_4	B_5H_5
BH^-	BH^-	9.75	19.96	26.56	1.257	1.097	0.939
BH	CH	10.87	25.21	33.62	1.063	0.932	0.742
BH	NH	17.18	31.31	40.43	0.969	0.871	0.786

		B−Y		
X[a]	Y[b]	B_3H_3	B_4H_4	B_5H_5
BH^-	BH^-	1.656	1.703	1.787
BH	CH	1.543	1.604	1.707
BH	NH	1.515	1.588	1.716

		B−B					
		D			WBI		
X[a]	Y[b]	B_3H_3	B_4H_4	B_5H_5	B_3H_3	B_4H_4	B_5H_5
BH^-	BH^-	1.869	1.842	1.787	0.395	0.466	0.536
BH	CH	1.936	1.847	1.781	0.262	0.370	0.443
BH	NH	2.017	1.878	1.820	0.200	0.330	0.396

[a] X = capping group with more diffuse orbital. [b] Y = capping group with less diffuse orbital. [c] θ = out-of-plane bending of the external B−H bonds of the B_nH_n, $n = 3-5$, ring toward Y.

Even though the B−Y bond lengths also vary, the B−B distances in these clusters remain nearly the same. The B−Y separations are 1.513, 1.555, and 1.680 Å in 1-NB_4H_5, 1-$CB_4H_5^-$, and $B_5H_5^{2-}$, respectively (Table 4). The B−X (X = BH) distance in 1-NB_4H_5 (1.655 Å) is shorter than in 1-$CB_4H_5^-$ and $B_5H_5^{2-}$ (1.666 and 1.680 Å, respectively).

Similar trends are found for other systems. The variation in BH out-of-plane bending with caps is related to the ring center to cap distance and B−Y distances for each cluster.[31] The comparison sets of 5-, 6-, and 7-vertex data in Table 4 reveal further relationships. These "inverse sandwiches" all have Y and X = BH caps, but the B_nH_n ring sizes vary from $n = 3$ to $n = 5$. The progression to the larger rings results in a greater degree of out-of-plane bending for Y = CH and Y = NH, the latter being larger. For a given cap, the B−Y distances get longer but the $B_{center}-Y$ distances get a bit shorter (with one minor exception). The change in ring size influences the BB distances (which get shorter in the ring but longer to the X = BH cap), but these are relatively unaffected by the nature of the Y cap. Our conclusions agree with expectations: a CH cap is more suitable than NH for four-membered and larger rings but NH is suitable for three-membered rings. Neither "fit" 5-rings well.

For example, the out-of-plane bending in the 8-vertex structures, composed of two layered three-membered boron rings and Y and X = BH caps, increases from $B_8H_8^{2-}$ (9.75°) to 1-$CB_7H_8^-$ (**8**) (10.87°) to 1-NB_7H_8 (**25**) (17.18°) (Table 5). The adjacent ring center to cap distance in $B_8H_8^{2-}$ (1.257 Å) decreases to 1.063A° in 1-$CB_7H_8^-$ and 0.969 Å in

1-NB_7H_8. The B−Y distances decrease from $B_8H_8^{2-}$ (1.656 Å) to 1-$CB_7H_8^-$ (1.543 Å) to 1-NB_7H_8 (1.515 Å). The smallest ring center to cap distance and the shortest B−Y bond are found in 1-NB_7H_8, which also has the largest out of plane bending (Table 5).

A similar trend is found in the 10-vertex systems (Table 5). While the out-of-plane bending is 19.96° in *closo*-$B_{10}H_{10}^{2-}$, it is 25.21° in 1-$CB_9H_{10}^-$ (**12**) and 31.31° in 1-NB_9H_{10} (**29**), as expected. The B_c−Y distance decreases from 1.097 Å ($B_{10}H_{10}^{2-}$) to 0.932 Å (1-$CB_9H_{10}^-$) to 0.871 Å (1-NB_9H_{10}). With less diffuse p-orbitals than carbon, nitrogen prefers a smaller ring in order to have optimum ring−cap overlap (Scheme 1c).

As the size of the borocycle ring increases, capping groups with more diffuse p-orbitals are needed to optimize the ring−cap interactions. Nitrogen, with its less diffuse orbitals, interacts poorly with the ring π-orbitals in the seven-vertex cage (Scheme 1b). This is reflected by out-of-plane bending in NB_6H_7 (Table 4). The ring hydrogens in 1-NB_6H_7 (**23**) are bent toward the cap (15.91°) more than in 1-CB_6H_7 (**5**) (8.96°), which has with more diffuse cap orbitals. The ring−cap distance, B−Y, in 1-NB_6H_7 is 1.759 Å, but it is longer, 1.830 Å, in $B_7H_7^{2-}$ (Table 4).

The BH out-of-plane hydrogens are bent toward the cap, which has less diffuse p-orbitals, independent of the B_nH_n ring (n = 3−5). This out-of-plane bending increases as the size of the ring increases (Table 4). For 1-NB_4H_5 with NH as the capping group, the out-of-plane bending is lower for the three-membered borocycle ring (8.19°) than the four- and five-membered borocycles (14.53° and 15.91°, respectively). This suggests that the ring hydrogens will be bent by large magnitudes toward the cap in five-membered rings. Hence, nitrogen with less diffuse p-orbitals is expected to prefer a smaller borocycle ring and should be unfavorable as a cap for larger rings.

The variations in out-of-plane bending for 12-vertex structures based on the five-membered borocycle (Table 5) are similar. The out-of-plane bending, 26.56°, calculated for *closo*-$B_{12}H_{12}^{2-}$ is less than the values of 33.62° and 40.43° calculated for *closo*-$CB_{11}H_{12}^-$ (**18**) and *closo*-$NB_{11}H_{12}$ (**35**), respectively. This indicates that BH, which has a more diffuse p-orbital, can optimize its interaction with the ring π-orbitals in the 12-vertex cage.

Thus, as shown in Table 5, for a cap combination involving nitrogen, the variations in the out-of-plane bending for the B_3H_3, B_4H_4, and B_5H_5 rings are 17.18° to 31.31° to 40.43°, as compared to the corresponding change from 10.87° to 25.21° to 33.62° for the CH cap.

The study of the relative energies of positional isomers of bipyramidal systems XYB_nH_n (X = BH, Y = CH, NH; n = 3−5) guides the selection of the appropriate ring for BH, CH, and NH as a cap. The relative energies of positional isomers of XYB_nH_n (X = BH, Y = CH, NH; n = 3−5) increase as the size of the borocycle ring increases (Tables 2 and 3).

There is a large difference in the relative energies of NB_6H_7 (**23**, 49.75 kcal/mol) and NB_4H_5 (**20**, 14.18 kcal/mol) (Table 3). The relative energy difference involving $CB_6H_7^-$ (**5**, 30.00 kcal/mol) and $CB_4H_5^-$ (**2**, 23.31 kcal/mol) is smaller (Table 2). This trend indicates that the best cap for a five-membered ring should be BH. The more diffuse boron p-

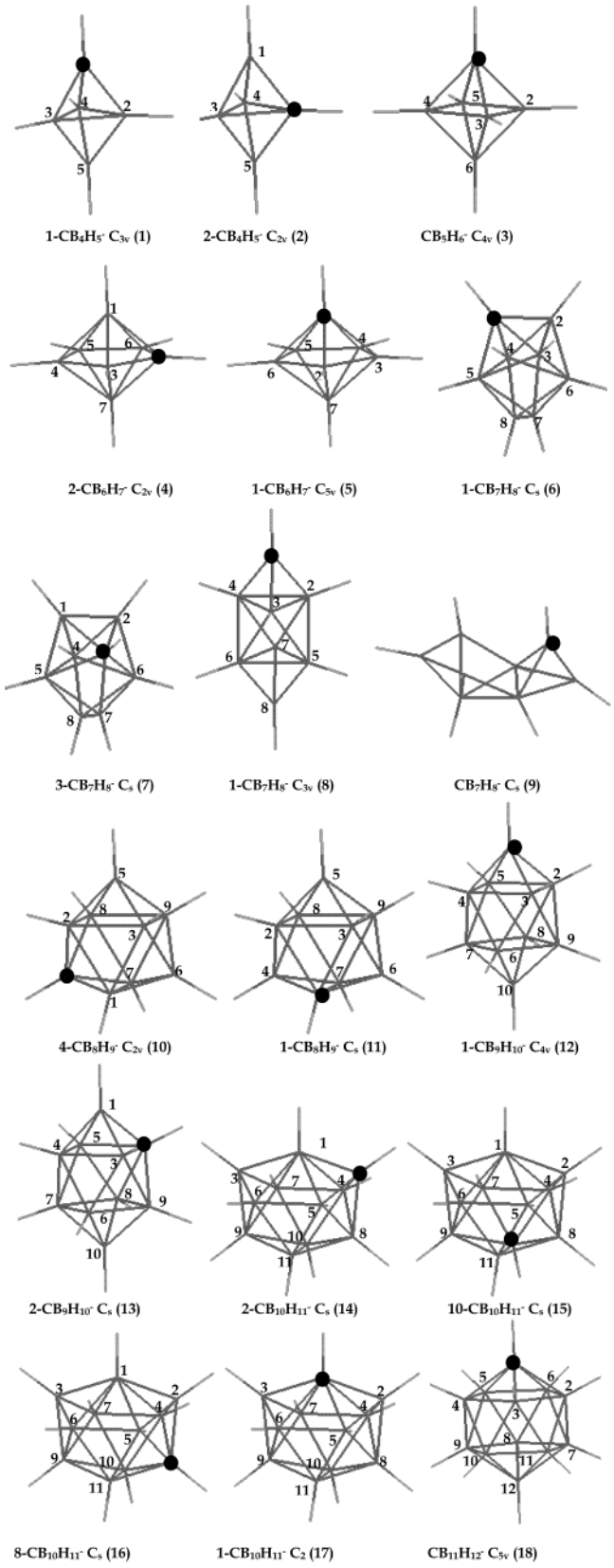

Figure 2. B3LYP/6-311+G** optimized for *closo*-monocarbaboranes $CB_{n-1}H_n^-$ (n = 5−12).

orbitals overlap best with the five-membered ring π-orbitals. A BH cap should be less satisfactory for three- and four-membered rings.

The relative energy of NB_4H_5 (**20**, 14.18 kcal/mol) is less than that of $CB_4H_5^-$ (**2**, 23.31 kcal/mol); this documents the preference of an NH cap for a three-membered ring relative to CH. The CH cap prefers a four-membered ring to three- and five-membered rings.

The same principles apply to bicapped "double-layer" systems. Thus, the C_{3v} structure of NB_7H_8 (**25**) is favored by its low-coordination nitrogen site, although this does not overcome the large, inherent 66.5 kcal/mol preference (see below) of the parent boron skeleton for D_{2d} over D_{3d} symmetry. The most stable NB_7H_8 isomer, **24**, is based on the D_{2d} skeleton but has a four-coordinate nitrogen. Nevertheless, **25** is favored over **26**, with its five-coordinate N. In contrast, the C_{3v} form of $CB_7H_8^-$ (**8**) (corresponding to **25**) is a high-energy minimum, even higher than the transition state 3-$CB_7H_8^-$ (**7**) (corresponding to **26**). Optimization of the other positional isomer of **8** with carbon on a center ring led to a *nido* form, **9**.

This study of bipyramidal systems clearly confirms the preference of a cap with less diffuse orbitals for a smaller ring, while caps with more diffuse orbitals prefer a larger ring.

Relative Energies of *closo*-Azaboranes, $NB_{n-1}H_n$ Isomers ($n = 5-12$). *closo*-Azaboranes $NB_{n-1}H_n$ ($n = 5-12$), closed polyhedral structures with triangular faces, are based on {BH} and {NH} units held together by multicenter bonding (Figure 3). The total coordination number (including the hydrogen) of cage vertex B or N atoms varies from 4 to 7. The total energies of all the *closo*-azaborane $NB_{n-1}H_n$ ($n = 5-12$) positional isomers are given in Table 3 along with the zero point energies and the number of imaginary frequencies. The *closo*-borane dianions, $B_nH_n^{2-}$ ($n = 5-12$), used as the reference framework for the natural charges on each vertex (calculated using NPA),[40] are shown in Figure 1 (along with the generally employed numbering scheme).

NB_4H_5. Although NB_4H_5 and its corresponding boron hydride, $B_5H_5^{2-}$, have never been reported experimentally, they are computed to have trigonal bipyramidal structures like that of the familiar isoelectronic *closo*-1,5-$C_2B_3H_5$, the smallest known 5-vertex carborane.[1-3]

As shown in Figure 1, apical sites 1 and 5 are four-coordinated, while the equatorial positions 2, 3, and 4 are five-coordinated. The empirical valence rules of Williams[28] predict that the 1-NB_4H_5 isomer (**19**) should be preferred over the 2-NB_4H_5 isomer (**20**) since nitrogen prefers sites with lower connectivity. According to the overlap criterion[31] (and as discussed in the previous section), three-membered rings also prefer NH rather than BH or CH as caps.

The charges in the parent reference frame, $B_5H_5^{2-}$ (Figure 1), are higher on the four-coordinated apical positions (−0.463) than on the five-coordinated equatorial sites (−0.260). According to Gimarc's topological charge stabilization rule,[29] the best placement of an electronegative heteroatom like nitrogen will be at the positions in the homoatomic system with the largest negative charge. As is apparent in the *closo*-borane dianion charges depicted in Figure 1, the lower coordination sites in all the species always have the more negative charges. When different sites have the same coordination (as in $B_5H_5^{2-}$ and $B_{11}H_{11}^{2-}$), the charges do not vary greatly.

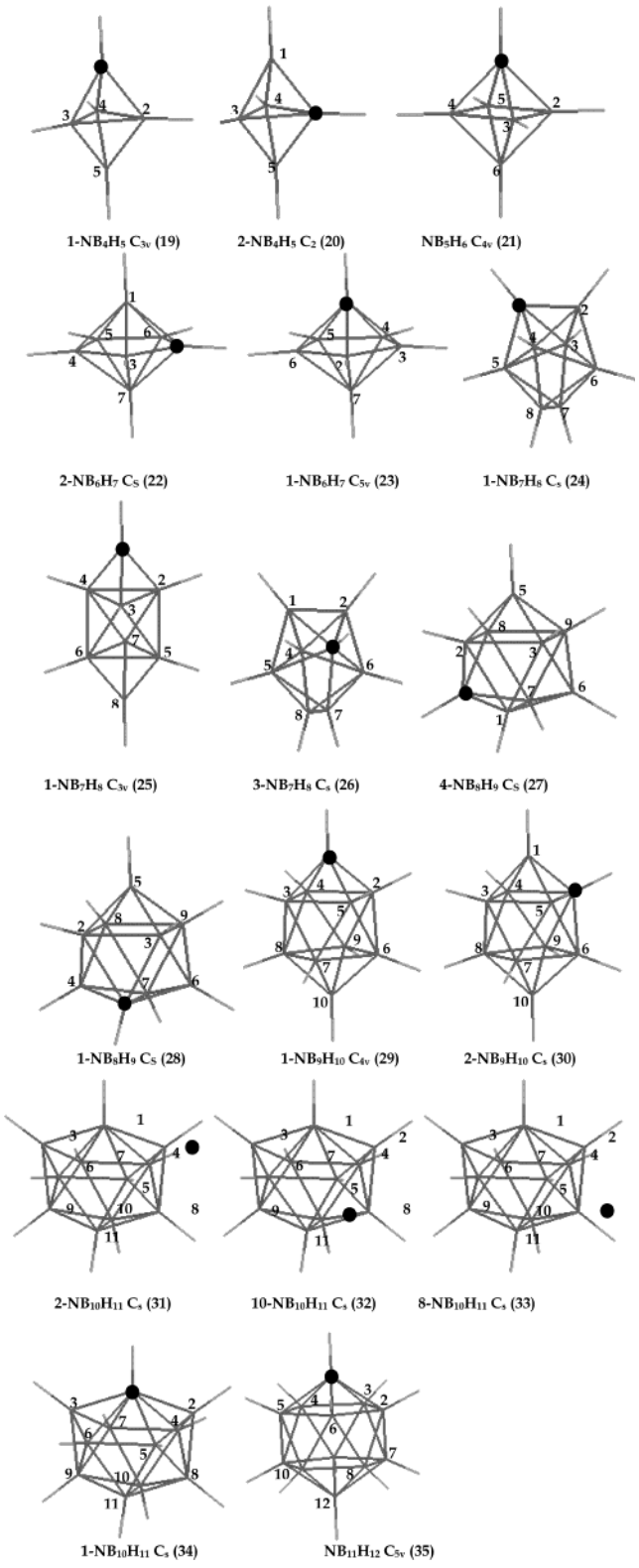

Figure 3. B3LYP/6-311+G** optimized for *closo*-azaboranes $NB_{n-1}H_n$ ($n = 5-12$).

All these considerations predict that 1-NB_4H_5 (**19**) will be more stable than 2-NB_4H_5 (**20**). Indeed, **19** is found to be the global 5-vertex minimum, whereas **20** is a higher order stationary point in C_{2v} symmetry (Table 3, Figure 3). Relaxation to lower symmetries results in a C_2 minimum (not shown). Our DFT 2-NB_4H_5 energies, relative to **19**, are C_2 (14.18 kcal/mol), C_s (48.28 kcal/mol), and C_{2v} (**20**, 48.13 kcal/mol) (Table 3).

NB_5H_6. Octahedral $B_6H_6^{2-}$ has six equivalent vertexes and a uniform charge distribution. There is only one NB_5H_6 isomer (Figure 3), a stable, C_{4v} minimum **(21)** (Table 3).

NB_6H_7. Although NB_6H_7 is not known, its structure should be based on the pentagonal bipyramid favored by the isoelectronic $B_7H_7^{2-}$.[1-3] Two aza isomers, 2-NB_6H_7 (**22**) and 1-NB_6H_7 (**23**), are possible. In contrast to $B_5H_5^{2-}$ (see Figure 1), the negative charges on the five-coordinated equatorial positions B2−B6 (−0.296) of the reference dianion $B_7H_7^{2-}$ are significantly more negative than the charge on the six-coordinated apical sites B1 and B7 (−0.107). Hence, **22** should be preferred over **23** (Table 3, Figure 3).

According to ring−cap matching criterion,[31] the B_5H_5 ring is more appropriate for a BH than a CH or NH cap. NH does not have orbitals diffuse enough to overlap effectively with the π-orbitals of a five-membered ring. Therefore, **22** should be more stable than **23** on all counts. Indeed, our DFT computations show 2-NB_6H_7 **(22)** to be 49.75 kcal/mol lower in energy than 1-NB_6H_7 **(23)**.

NB_7H_8. Although NB_7H_8 is not known, its structure is likely to be a slightly distorted dodecahedron based on the D_{2d} symmetry favored by the isoelectronic borane $B_8H_8^{2-}$ dianion.[36] Although a second $B_8H_8^{2-}$ form has D_{3d} symmetry and offers two four-coordinate cap sites, it has two imaginary frequencies and is 66.5 kcal/mol higher in energy than the D_{2d} form. The equivalent five-coordinate positions 1, 2, 7, and 8 (Figure 1) bear more negative charges (−0.289) than the six-coordinated sites, 3, 4, 5, and 6 (−0.141). Hence, 1-NB_7H_8 **(24)** should be preferred over 3-NB_7H_8 **(26)**, also on the basis of the connectivity.

We find 1-NB_7H_8 (**24**, C_s) to be the global 8-vertex minimum (Table 3); 3-NB_7H_8 (**26**, C_s) (Figure 3) has one imaginary frequency and is 20.61 kcal/mol higher in energy. We examined the C_{3v} symmetry NB_7H_8 form (**25**), based on the D_{3d} $B_8H_8^{2-}$ mentioned above. It proved to be a minimum, but was 15.90 kcal/mol higher in energy than **24**. When a nitrogen is placed at one of the 6-cordinate sites of D_{3d} $B_8H_8^{2-}$, optimization leads to the most stable isomer, 1-NB_7H_8 **(24)**.

NB_8H_9. Although NB_8H_9 has never been prepared, its structure should be based on the tricapped trigonal $B_9H_9^{2-}$ prism (Figure 1). Note that the three vertexes (4, 5, and 6), which cap the rectangular faces of the $B_9H_9^{2-}$ prism, are five-coordinated and carry a larger negative charge (−0.347) than the six-coordinate prism vertexes (−0.129). Therefore, the 4-NB_8H_9 isomer **(27**) should be more stable than 1-NB_8H_9 **(28)**. The computations agree; the energy difference is 14.60 kcal/mol (Table 3). While 1-NB_8H_9 (C_s) **(27**) is a minimum, **28** in C_{2v} symmetry is not; symmetry relaxation hardly changes the energy, but optimization results in the C_s global minimum, **27** (Figure 3). Likewise, optimization of 4-NB_8H_9 in C_{2v} symmetry did not lead to a significant energy difference from 1-NB_8H_9 (C_s).

NB_9H_{10}. The experimentally known[37,38] C_{4v} 1-NB_9H_{10} **(29)** and the C_s 2-NB_9H_{10} **(30)** minima (Figure 3) are based on the isoelectronic $B_{10}H_{10}^{2-}$ bicapped square antiprism. The negative (−0.285) charges of the five-coordinated square face capping sites 1 and 10 contrast with those (−0.171) of the eight six-coordinated B's. Hence, on the basis of both charge topology and connectivity considerations, it is not surprising that **29** is 33.00 kcal/mol lower in energy than **30** (Table 3).[39]

$NB_{10}H_{11}$. The $NB_{10}H_{11}$ isomers, all unknown, can be derived from the isoelectronic C_{2v} $B_{11}H_{11}^{2-}$ (see Figure 2). The latter offers one seven-, two equivalent five-, and eight six-coordinated positions (in sets of 4, 2, and 2). The empirical valence rules of Williams locate nitrogen at sites with lower connectivity and predict the stability order 2-$NB_{10}H_{11}$ (**31**) > 10-$NB_{10}H_{11}$ (**32**) ∼ 8-$NB_{10}H_{11}$ (**33**) > 1-$NB_{10}H_{11}$ (**34**). The same order is predicted by the charges shown for C_{2v} $B_{11}H_{11}^{2-}$ in Figure 2. The computed energies agree.

Geometry optimization on all the positional isomers of $NB_{10}H_{11}$ located C_s symmetry minima for 2-$NB_{10}H_{11}$ **(31)**, 10-$NB_{10}H_{11}$ **(32)**, and 8-$NB_{10}H_{11}$ **(33)** (Figure 3). Relative to 2-$NB_{10}H_{11}$ **(31)**, the energies of **32** and **33** are 32.61 and 36.48 kcal/mol, respectively (Table 3). In contrast, 1-$NB_{10}H_{11}$ **(34)** has two imaginary frequencies in C_s symmetry (Table 3) and a relative energy of 40.42 kcal/mol. Optimization without symmetry constraints leads to the global minimum, **31**. The same is true with the 4-$NB_{10}H_{11}$ starting geometry.

$NB_{11}H_{12}$. Because of the icosahedral geometry of the parent dianion, $B_{12}H_{12}^{2-}$, only one closo $NB_{11}H_{12}$ isomer **(35)** with C_{5v} geometry is possible (Table 3, Figure 3). It is a stable minimum, in agreement with experimental and earlier theoretical studies.[45,27]

Stability of the *closo*-Azaboranes, $NB_{n-1}H_n$ ($n = 5-12$). Recently, we assessed[10] the stabilization energies as well as the average energy per CH group in two-dimensional aromatic compounds. The Hückel annulenes behave differently from the polybenzenoid hydrocarbons.[10] The strain-corrected total aromatic stabilization energies (ASE) of the Hückel annulenes do not increase with increasing ring size; hence, the average stability per π electron (or CH group) decreases, e.g., the energy and the aromatic stabilization energies of $C_{18}H_{18}$ are much less than those of three benzenes.[10] In contrast, the total aromatic stabilization energies of polybenzenoid hydrocarbons increase with size. Although there are variations, one can generalize that the average energy per π electron (or CH group) is constant or

(42) (a) Buhl, M.; Mebel, A. M.; Charkin, O. P.; Schleyer, P. v. R. *Inorg. Chem.* **1992**, *31*, 3769. (b) Bausch, J. W.; Prakash, G. K. S.; Williams, R. E. *Inorg. Chem.* **1992**, *31*, 3763. (c) Kleir, D. A.; Lipscomb, W. N. *Inorg. Chem.* **1979**, *18*, 1312. (d) Muetterties, E. L.; Wiersama, R. J.; Hawthorne, M. F. *J. Am. Chem. Soc.* **1973**, *95*, 7520.
(43) Schneider, L.; Englert, U.; Paetzold, P. *Z. Anorg. Allg. Chem.* **1994**, *620*, 1191.
(44) Buhl, M.; Schleyer, P. v. R.; Havals, Z.; Hynk, D.; Hermanek, S. *Inorg. Chem.* **1991**, *30*, 3107.
(45) Zahradnik, R.; Balaji, V.; Michl, J. *J. Comput. Chem.* **1991**, *12*, 1147.

only falls off somewhat. [10,46−49] We have pointed out that both these types of two-dimensional aromatic systems behave quite differently from the "three-dimensional aromatic" (*closo*-borane-based) clusters.[10]

Both the total stabilization energies of the *closo*-borane dianions and also the average stability per vertex tend to become larger with increased cluster size. This is true for the most stable positional isomers of the *closo*-monocarbaborane anions, $CB_{n-1}H_n^-$ ($n = 5-12$), the *closo*-dicarboranes, $C_2B_{n-2}H_n$ ($n = 5-12$), and the isoelectronic, *closo*-borane dianions, $B_nH_n^{2-}$ ($n = 5-12$).[30] The stabilities of these three sets of clusters generally increase with increasing cluster size from 5 to 12 vertexes. There are variations in the stabilities of individual members of each set, but these also show quite similar trends. The exceptional energetic behavior of *closo*-$B_nH_n^{2-}$, *closo*-$CB_{n-1}H_n^-$, and the *closo*-$C_2B_{n-2}H_n$ family is a direct indication of three-dimensional aromaticity.[30] Unlike the Hückel aromatics, the stabilities become proportionately greater with increasing cluster size. But this is true only up to 12 vertex systems; larger three-dimensional clusters are less stable due to the nonoptimal bonding.[3,9a,10a,30]

We now extend our evaluation of the cluster stabilization of related families to a new member, the *closo*-azaboranes, $NB_{n-1}H_n$ ($n = 5-12$). Their energies can be compared with those for the *closo*-borane dianions, $B_nH_n^{2-}$ ($n = 5-12$), and the *closo*-monocarbaborane anions, $CB_{n-1}H_n^-$ ($n = 5-12$), by means of eqs 1−3.

$$B_2H_2^{2-} + (n-2)BH_{increment} \rightarrow B_nH_n^{2-}\ (n = 5-12) \qquad \Delta H \quad (1)$$

$$CBH_2^- + (n-1)BH_{increment} \rightarrow CB_nH_{n+1}^-\ (n = 4-11) \qquad \Delta H \quad (2)$$

$$NBH_2 + (n-1)BH_{increment} \rightarrow NB_nH_{n+1}\ (n = 4-11) \qquad \Delta H \quad (3)$$

Data for the most stable positional isomers are used for the last two sets. The $BH_{increment}$ is taken as the difference in energy between B_3H_5 (C_{2v}, planar) and B_2H_4 (D_{2h}). $B_2H_2^{2-}$, CBH_2^-, and NBH_2 are assumed to have acetylene-like structures. The BH increment is obtained from molecules in which there is no inherent delocalization or hyperconjugation.

As summarized in Tables 1, 7, and 8, all the reaction energies (ΔH) of eqs 1−3 are exothermic. Figure 4 shows that ΔH tends to increase with increasing cluster size. This plot emphasizes our earlier conclusions[3c,10a,30] for the 5 to 12 clusters: (a) the trend toward increasing stability with cluster size and (b) the individual variations in the three sets of clusters.

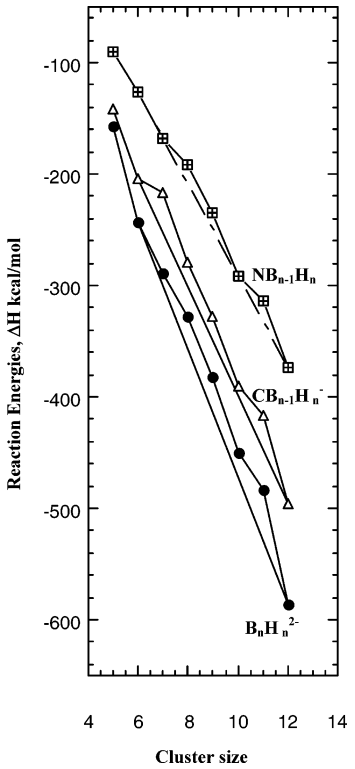

Figure 4. Plot of the reaction energies, ΔH in kcal/mol, of the *closo*-borane dianions, $B_nH_n^{2-}$, and the most stable $CB_{n-1}H_n^-$ and *closo*-azaboranes $NB_{n-1}H_n$ from Tables 1, 7, and 8 vs cluster size. The trends to more negative ΔH's are shown by the lines defined by the 6- and 12-vertex systems in each family. The deviations from the lines are largest for *closo*-borane dianions, $B_nH_n^{2-}$, smallest for *closo*-azaboranes, $NB_{n-1}H_n$ ($n = 5-12$), and intermediate for the *closo*-monocarbaborane $CB_{n-1}H_n^-$ set.

Table 6. HOMO−LUMO Gap (kcal/mol) of *closo*-Borane Dianions, $B_nH_n^{2-}$, the Most Stable *closo*-Monocarbaboranes, $CB_{n-1}H_n^-$, and the Most Stable *closo*-Azaboranes, $NB_{n-1}H_n$, Calculated at the B3LYP/6-311+G** Level

	H−L		
cluster	$B_nH_n^{2-}$	$CB_{n-1}H_n^-$	$NB_{n-1}H_n$
5 vertex	41.29	108.33	155.34
6 vertex	107.27	168.80	159.88
7 vertex	69.62	119.99	142.08
8 vertex	53.68	110.96	124.82
9 vertex	65.10	119.43	124.34
10 vertex	83.62	134.97	150.00
11 vertex	75.99	150.28	112.92
12 vertex	117.00	153.19	174.89

Equation 1 gives the largest exothermicities (Figure 4), but these results are influenced strongly by Coulomb interaction effects. $B_2H_2^{2-}$ is highly energetic due to the repulsion of the two adjacent negative charges, but this decreases as the *closo*-$B_nH_n^{2-}$ become larger. The charges are delocalized and separated to a greater degree. The plots in Figure 4 are based on the data treatment used previously to evaluate the relative stability of *closo*-borane dianions, $B_nH_n^{2-}$ ($n = 5-12$), and *closo*-monocarbaborane anions, $CB_{n-1}H_n^-$ ($n = 5-12$), which we have extended to the *closo*-azaborane, $NB_{n-1}H_n$ ($n = 5-12$), systems. Data from eqs 1−3 for the most symmetrical 6- and 12-vertex species are used to define the reference lines in Figure 4: deviations from the line (ΔH_{dev},[44] Table 9) were used for the quantitative comparison of the stabilities of individual clusters.

(46) Roth, W. R.; Hopf, H.; Wasser, T.; Zimmermann, H.; Werner, C. *Liebigs Ann.* **1996**, 1691.
(47) Aihara, J. *J. Chem. Soc., Perkin Trans. 2* **1996**, 2185.
(48) Peck, R. C.; Schulman, J. M.; Disch, R. L. *J. Phys. Chem.* **1990**, *94*, 6637.
(49) Wiberg, K. B. *J. Org. Chem.* **1997**, *62*, 5720.

Table 7. Most Stable *closo*-Monocarbaborane Anions, $CB_{n-1}H_n^-$ (n = 5−12): Total Energies (au), Zero Point Energies (ZPE, kcal/mol),[a] and Reaction Energies from Eq 2 (ΔH)[b]

molecule	sym	ZPE[a]	B3LYP/6-311+G**	ΔH[b]
1-$CB_4H_5^-$	C_{3v}	41.33	−140.58607	−141.96
$CB_5H_6^-$	C_{4v}	51.43	−166.101098	−204.11
2-$CB_6H_7^-$	C_{2v}	60.55	−191.53629	−246.97
1-$CB_7H_8^-$	C_s	69.33	−217.04977	−279.62
4-$CB_8H_9^-$	C_{2v}	78.70	−242.54224	−328.33
1-$CB_9H_{10}^-$	C_{4v}	89.98	−268.05625	−389.67
2-$CB_{10}H_{11}^-$	C_s	97.41	−93.51193	−416.23
$CB_{11}H_{12}^-$	C_{5v}	108.81	−319.05723	−496.09

[a] Zero point energies (ZPE, kcal/mol), calculated at B3LYP/6-31G*. [b] $CBH_2^- + (n-1)BH_{increment} \rightarrow CB_nH_{n+1}^-$ (n = 4−11) at B3LYP/6-311+G**, with ZPE corrections (ref 39) scaled by 0.98 in kcal/mol.

Table 8. Most Stable *closo*-Azaboranes, $NB_{n-1}H_n$ (n = 5−12): Total Energies (au),[a] Zero Point Energies (ZPE, kcal/mol), and Reaction Energies from Eq 3 (ΔH)[b]

molecule	sym	ZPE[a]	B3LYP/6-311+G**	ΔH[b]
1-NB_4H_5	C_{3v}	43.24	−157.22270	−90.78
NB_5H_6	C_{4v}	52.50	−182.69360	−126.08
2-NB_6H_7	C_s	61.29	−280.17426	−167.95
1-NB_7H_8	C_s	70.13	−233.62703	−192.29
4-NB_8H_9	C_1	79.70	−259.10899	−234.22
1-NB_9H_{10}	C_{4v}	89.98	−284.61614	−291.25
2-$NB_{10}H_{11}$	C_s	98.09	−310.06449	−313.54
$NB_{11}H_{12}$	C_{5v}	108.76	−335.57682	−373.43

[a] Zero point energies (ZPE, kcal/mol), calculated at B3LYP/6-31G*. [b] $NBH_2 + (n-1)BH_{increment} \rightarrow NB_nH_{n+1}$ (n = 4−11) at B3LYP/6-311+G**, with ZPE corrections (ref 39) scaled by 0.98 in kcal/mol.

Table 9. Deviations (ΔH_{dev}, in kcal/mol) of *closo*-Borane Dianions, $B_nH_n^{2-}$,[a] the Most Stable *closo*-Monocarbaboranes, $CB_{n-1}H_n^-$,[b] and the Most Stable *closo*-Azaboranes, $NB_{n-1}H_n$,[c] from the Lines Defined by the 6- and 12-Vertex Species (see Figure 4)

cluster	ΔH_{dev}[a] $B_nH_n^{2-}$	ΔH_{dev}[b] $CB_{n-1}H_n^-$	ΔH_{dev}[c] $NB_{n-1}H_n$
5 vertex	28.45	13.48	−5.93
6 vertex	0.00	0.00	0.00
7 vertex	11.56	5.80	−0.65
8 vertex	29.08	21.81	16.24
9 vertex	31.90	21.76	15.53
10 vertex	22.06	9.09	−0.27
11 vertex	45.70	31.19	18.67
12 vertex	0.00	0.00	0.00

[a] Calculated using eq 1. [b] Calculated using eq 2. [c] Calculated using eq 3.

The variation patterns (ΔH_{dev}) of corresponding compounds are extremely similar qualitatively in the *closo*-borane dianions, $B_nH_n^{2-}$ (n = 5−12), *closo*-monocarbaborane anions, $CB_{n-1}H_n^-$ (n = 5−12), and *closo*-azaborane, $NB_{n-1}H_n$ (n = 5−12), clusters. As shown in Figure 4 and Table 9, the quantitative deviations from the defining lines are greatest for the *closo*-borane dianions, $B_nH_n^{2-}$, less for *closo*-monocarbaborane anions, $CB_{n-1}H_n^-$ (n = 5−12), and least for the *closo*-azaboranes, $NB_{n-1}H_n$. The deviations (ΔH_{dev}) of the *closo*- $B_nH_n^{2-}$ clusters are the largest of the three sets. $B_{11}H_{11}^{2-}$ has the largest deviation, ΔH_{dev} = 45.70 kcal/mol, while the $B_7H_7^{2-}$ has the smallest, ΔH_{dev} = 11.56 kcal/mol. $B_5H_5^{2-}$, $B_8H_8^{2-}$, and $B_9H_9^{2-}$ deviations are ΔH_{dev} = 28.54, 29.08, and 31.90 kcal/mol, respectively.

The ΔH_{dev} values for clusters with the same number of vertexes decrease from *closo*-borane dianions, $B_nH_n^{2-}$, to *closo*-monocarbaborane anions, $CB_{n-1}H_n^-$, and from *closo*-monocarbaborane anions, $CB_{n-1}H_n^-$, to *closo*-azaboranes, $NB_{n-1}H_n$ (Table 9). For example, the ΔH_{dev} values for the 8- and 9-vertex *closo*-$B_nH_n^{2-}$ (29.08 and 31.90 kcal/mol, respectively) are more than those of *closo*-$CB_{n-1}H_n^-$ (21.81 and 21.76 kcal/mol, respectively) and decrease further in *closo*-$NB_{n-1}H_n$ (to 16.24 and 15.53 kcal/mol, respectively).

These leveling effects, relative to *closo*-$B_nH_n^{2-}$, in the *closo*-$CB_{n-1}H_n^-$ family and even more in the *closo*-$NB_{n-1}H_n$ set, are due to the partial electron localization due to the more electronegative heteroatoms, carbon and especially nitrogen. The magnitude of these leveling effects is more than twice as large for the *closo*-azaborane $NB_{n-1}H_n$ families as for the *closo*-$CB_{n-1}H_n^-$ set. Obviously, the larger electron localization at nitrogen is due to its greater electronegativity.

Support for this rationalization also is found, e.g., in the variations and trends in the HOMO−LUMO gaps (Table 6), in the Wiberg bond indexes (WBI), and in the C−B and N−B distance ranges from the *closo*-$B_nH_n^{2-}$ to the *closo*-$CB_{n-1}H_n^-$ and from the *closo*-$CB_{n-1}H_n^-$ to the *closo*-$NB_{n-1}H_n$ sets (Tables 4 and 5).

The quantitative variation in B−B Wiberg bond indices (WBI), a measure of the bonding interactions between the BB in the borocycle ring, are greatest for the $B_nH_n^{2-}$, less for the $CB_{n-1}H_n^-$, and least for the $NB_{n-1}H_n$ set. This also is a consequence of the greater electron localization at the electronegative nitrogen. Accordingly, the WBI values of $B_5H_5^{2-}$ (0.462) are larger than those of $CB_4H_5^-$ and NB_4H_5 (0.373 and 0.369) (Table 4). Note the same trend in the 6-vertex systems: the WBIs for $B_6H_6^{2-}$, 1-$CB_4H_5^-$, and 1-NB_4H_5 vary from 0.683 to 0.600 to 0.572, respectively (Table 4).

Similar decreases in the BB WBIs are found in the 10- and 12-vertex species (Table 5), e.g., going from $B_{10}H_{10}^{2-}$ (0.466) to 1-$CB_9H_{10}^-$ (0.370) (nearest the heteroatoms) to 1-NB_9H_{10} (0.330). The WBI decreases from WBI = 0.536 for $B_{12}H_{12}^{2-}$ to WBI = 0.396 for $NB_{11}H_{12}$.

Leveling effects also are shown by HOMO−LUMO gaps of the cluster sets. These gaps for clusters with the same number of vertexes increase from *closo*-$B_nH_n^{2-}$ to *closo*-$CB_{n-1}H_n^-$ and from *closo*-$CB_{n-1}H_n^-$ to *closo*-$NB_{n-1}H_n$ (Table 6). The *closo*-$NB_{n-1}H_n$ has the largest HOMO−LUMO gap because of greater electronegativity of nitrogen. For example, the HOMO−LUMO gap in $B_5H_5^{2-}$ is 41.29 kcal/mol, while the corresponding energies in 1-$CB_4H_5^-$ and 1-NB_4H_5 are 108.33 and 155.34 kcal/mol, respectively. Likewise, the 142.08 kcal/mol gap in *closo*-NB_6H_7 is larger in magnitude than that of *closo*-$B_7H_7^{2-}$ and *closo*-$CB_6H_7^-$ (69.62 and 119.99 kcal/mol, respectively). A similar trend is found in the 8-, 9-, 10-, and 12-vertex systems, where the *closo*-azaborane representatives have the largest HOMO−LUMO gaps (Table 6).

Further leveling effects are shown by the B−Y (Y = CH, NH) distances. Among the 5-, 6-, and 7-vertex clusters, *closo*-$B_nH_n^{2-}$ has the largest B−Y distance and *closo*-$NB_{n-1}H_n$ has the smallest (Table 4). The same trend is found in 8-, 10-, and 12-vertex clusters (Table 5).

Three-Dimensional Aromaticity in *closo*-Azaboranes, $NB_{n-1}H_n$ (n = 5−12). Aromaticity[51,52] is often evaluated

by using various criteria: energetic (resonance energies, aromatic stabilization energies (ASE)),[53,54] magnetic (^{1}H NMR chemical shifts,[55] magnetic susceptibility anisotropies[56] and exaltations, Λ,[37] as well as NICS[36]), and geometric (bond length equalization, bond order indices).[57,58] The diamagnetic and paramagnetic effects of the ring current associated with the aromaticity and antiaromaticity are measured by the simple and efficient NICS criterion. NICS, proposed by Schleyer and co-workers,[36] is based on the negative absolute magnetic shielding computed at the cluster centers or above the centers of the rings. NICS is widely employed to characterize aromaticity and antiaromaticity of both ring systems and three-dimensional clusters.[59,60] Negative NICS values (given in ppm) imply aromaticity (diatropic ring currents), and positive NICS values correspond to antiaromaticity (paratropic ring currents). In contrast to other aromaticity criteria, NICS does not require reference molecules, increment schemes, or equations for evaluation.[36] While excellent correlation among NICS with other aromaticity indexes based on geometric, energetic, and other magnetic criteria has been demonstrated,[61,62] such quantitative relationships did not extend to more complex systems when other effects dominated. We will now apply these criteria (with special emphasis on the magnetic properties) to the question of aromaticity in the *closo*-azaborane $NB_{n-1}H_n$ ($n = 5-12$).

Table 10. Nucleus Independent Chemical Shifts (NICS, ppm) of *closo*-Borane Dianions, $B_nH_n^{2-}$,[a] the Most Stable *closo*-Monocarbaboranes, $CB_{n-1}H_n^-$,[b] and the *closo*-Azaboranes, $NB_{n-1}H_n$[c]

cluster	$B_nH_n^{2-}$ [a]	$CB_{n-1}H_n^-$ [b]	$NB_{n-1}H_n$[c]
5 vertex	−23.08	−17.42	−12.46
6 vertex	−26.51	−26.64	−25.88
7 vertex	−19.73	−20.32	−15.65
8 vertex	−16.67	−16.77	−14.72
9 vertex	−21.07	−20.15	−16.69
10 vertex	−27.52	−24.85	−19.96
11 vertex	−26.24	−24.00	−19.44
12 vertex	−28.44	−28.00	−26.30

[a−c] At CSGT-B3LYP/6-311+G**//B3LYP/6-311+G**.

The three-dimensional aromatic delocalization of *closo*-borane dianions, $B_nH_n^{2-}$ ($n = 5-12$),[10] *closo*-monocarbaborane anions, $CB_{n-1}H_n^-$ ($n = 5-12$), and *closo*-dicarboranes, $C_2B_{n-2}H_n$ ($n = 5-12$), was demonstrated by the large negative NICS values and the magnetic susceptibility exaltations.[30] However, the aromaticity ordering based on these magnetic properties does not always agree with the relative stabilities of positional isomers of the same cluster;[30] this shows that other effects such as connectivity and charge considerations are important.[34a,35]

Nucleus Independent Chemical Shift of *closo*-Azaboranes, $NB_{n-1}H_n$ ($n = 5-12$). The large NICS values at the cage centers of *closo*-azaboranes, $NB_{n-1}H_n$ ($n = 5-12$), −26.30 to −12.46 ppm, document the pronounced "three-dimensional delocalization" (Table 10). As functions of cluster size, NICS of the *closo*-borane dianions, $B_nH_n^{2-}$ ($n = 5-12$), the *closo*-monocarbaborane anions, $CB_{n-1}H_n^-$ ($n = 5-12$), and the *closo*-azaboranes, $NB_{n-1}H_n$ ($n = 5-12$), show similar patterns (Figure 5). The $B_nH_n^{2-}$ NICS values are largest among the three sets, but not in every case. The highest symmetry 6- and 12-vertex polyhedra are the most "aromatic" in each family. Thus, NB_5H_6 (NICS −25.88) and $NB_{11}H_{12}$ (−26.30) have the largest and NB_5H_6 has the smallest NICS (−12.46) among the *closo*-azaboranes; the others range from −14.72 (8-vertex) to −19.96 (10-vertex) (Table 10).

Magnetic Susceptibility Exaltation, Λ of *closo*-Azaboranes, $NB_{n-1}H_n$ ($n = 5-12$). The magnetic susceptibility exaltation (Λ) is a manifestation of ring currents arising from cyclic electron delocalization. Generally Λ is defined as the difference between the bulk magnetic susceptibility (χ_m) of a compound and the susceptibility (χ'_m) estimated from an increment system or from model compounds without cyclic conjugation.[37] Aromatic compounds are characterized by negative Λ's, whereas antiaromatic compound show positive Λ's. As anticipated by Lipscomb,[4c] negative Λ's also characterize three-dimensional aromaticity in *closo* clusters. Λ's are evaluated here using eqs 1−3 for the *closo*-borane dianions, $B_nH_n^{2-}$, *closo*-monocarbaborane anions, $CB_{n-1}H_n^-$, and *closo*-azaboranes, $NB_{n-1}H_n$, at the CSGT-B3LYP/6-311+G**//B3LYP/6-311+G** level (Table 11). The Λ values show *closo*-azaboranes, $NB_{n-1}H_n$, to be "three-dimensional aromatics" just like the corresponding *closo*-

(50) The estimated reaction energies for each *closo*-borane dianion $B_nH_n^{2-}$ can be evaluated by $\Delta H_{estimated} = 100.56 - 57.218x$ (where x is the number of vertexes). This equation defines the straight line which connected the two reference species $B_{12}H_{12}^{2-}$ and $B_6H_6^{2-}$ in Figure 4. Hence, the deviation of the energy of each cluster from this line (ΔH_{dev}) can be estimated by taking the differences between ΔH_{est} and the reaction energies from eq 1 (ΔH_{obs}) (Table 1), $\Delta H_{dev} = \Delta H_{est} - \Delta H_{obs}$.

(51) (a) Jug, K.; Koster, A. M. *J. Phys. Org. Chem*. **1991**, *4*, 163. (b) Katritzky, A. R.; Feygelman, V.; Musumarra, G.; Barczynski, P.; Szafran, M. *J. Prakt. Chem./Chem.-Ztg*. **1990**, 332, 835. (c) Katritzky, A. R.; Barczynski, P.; Musumarra, G.; Pisano, D.; Szafran, M. *J. Am. Chem. Soc*. **1989**, *111*, 7. (d) Garret, P. J. *Aromaticity*; Wiley: New York, 1986.

(52) (a) Krygowski, T. M.; Cyranski, M. K.; Czarnocki, Z.; Hafelinger, G.; Katritzky, A. R. *Tetrahedron* **2000**, *56*, 1783. (b) Schleyer, P. v. R.; Jiao, H. *Pure Appl. Chem*. **1996**, *68*, 209. (c) Bird, C. W. *Tetrahedron* **1996**, *52*, 9945. (d) Minkin, V. I.; Glukhovtsev, M. N.; Simkin, B. Y. *Aromaticity and Antiaromaticity*; Wiley: New York, 1994.

(53) (a) Hess, B. A., Jr.; Schaad, L. J. *J. Am. Chem. Soc*. **1971**, *93*, 305. (b) Dewar, M. J. S.; De Llano, C. *J. Am. Chem. Soc*. **1969**, *91*, 789.

(54) (a) Gutman, I.; Milun, M.; Trinajstic, N. *J. Am. Chem. Soc*. **1977**, *99*, 1692. (b) Aihara, J. *J. Am. Chem. Soc*. **1976**, *98*, 2750.

(55) Elvidge, J. A.; Jackman, L. M. *J. Chem. Soc*. **1961**, 859.

(56) (a) Fleischer, U.; Kutzelnigg, W.; Lazzeretti, P.; Muhlenkamp, V. *J. Am. Chem. Soc*. **1994**, *116*, 5296 and references therein. (b) Benson, R. C.; Flygare, W. H. *J. Am. Chem. Soc*. **1970**, *92*, 7253.

(57) (a) Herndon, W. C. *J. Am. Chem. Soc*. **1973**, *95*, 2404. (b) Kruszewski, J.; Krygowski, T. M. *Tetrahedron Lett*. **1972**, 3839. (c) Jug, A.; Francois, P. *Theor. Chim. Acta* **1967**, *7*, 249.

(58) (a) Bird, C. W. *Tetrahedron* **1985**, *41*, 1409. (b) Jug, K. *J. Org. Chem*. **1983**, *48*, 1344. (c) Aihara, J. *J. Org. Chem*. **1976**, *41*, 2488.

(59) (a) Patchkovskii, S.; Thiel, W. *J. Mol. Model*. **2000**, *6*, 67 and references cited. (b) Sawicka, D.; Wilsey, S.; Houk, K. N. *J. Am. Chem. Soc*. **1999**, *121*, 864. (c) Buhl, M. *Chem. Eur. J*. **1998**, *4*, 734.

(60) (a) Lera, A. R.; Alvarez, R.; Lecea, B.; Torrado, A.; Cossio, F. P. *Angew. Chem., Int. Ed*. **2001**, *40*, 557. (b) Verevkin, S. P.; Beckhaus, H.-D.; Ruckhardt, C.; Haag, R.; Kozhushkov, S. I.; Zywietz, T.; de Meijere, A.; Jiao, H.; Schleyer, P. v. R. *J. Am. Chem. Soc*. **1998**, *120*, 11130.

(61) (a) Nyulaszi, L.; Schleyer, P. v. R. *J. Am. Chem. Soc*. **1999**, *121*, 6872. (b) Chesnut, D. B. *Chem. Phys*. **1998**, *231*, 1.

(62) (a) Krygowski, T. M.; Cyranski, M. K. *Chem. Rev*. **2001**, *101*, 1385. (b) Abraham, R. J.; Canton, M.; Reid, M.; Griffiths, L. *J. Chem. Soc., Perkin Trans. 2* **2000**, 803.

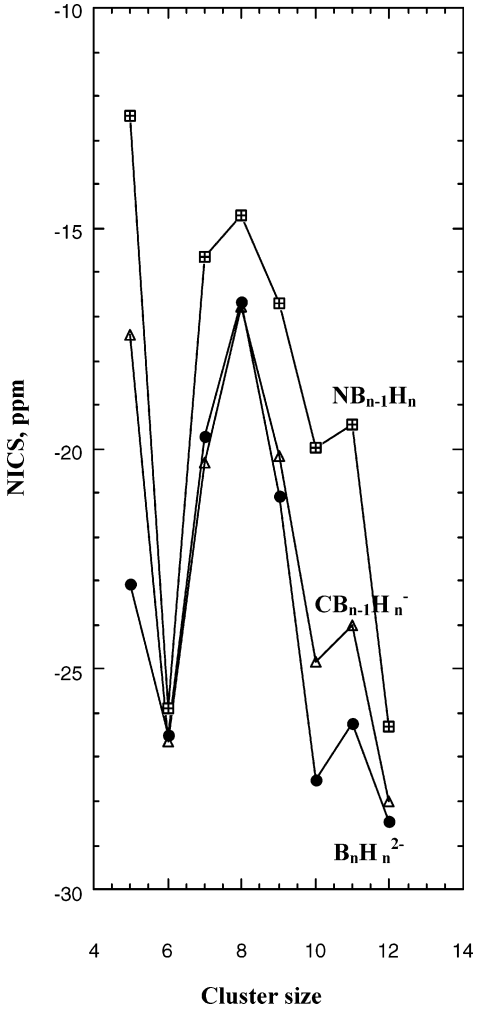

Figure 5. Plot of NICS at the center of *closo*-$B_nH_n^{2-}$ and the most stable *closo*-$CB_{n-1}H_n^-$ and *closo*-$NB_{n-1}H_n$ (from Table 10) vs cluster size.

Table 11. Magnetic Susceptibility Exaltations (Λ, ppm cgs) of *closo*-Borane Dianions, $B_nH_n^{2-}$,[a] the Most Stable *closo*-Monocarbaboranes, $CB_{n-1}H_n^-$,[b] and the *closo*-Azaboranes, $NB_{n-1}H_n$[c]

cluster	$B_nH_n^{2-}$ [a]	$CB_{n-1}H_n^-$ [b]	$NB_{n-1}H_n$[c]
5 vertex	−33.49	−32.38	−28.02
6 vertex	−45.01	−49.79	−47.46
7 vertex	−49.23	−58.25	−52.13
8 vertex	−59.10	−67.52	−63.68
9 vertex	−83.76	−87.57	−80.22
10 vertex	−110.21	−109.94	−100.10
11 vertex	−115.66	−119.01	−110.52
12 vertex	−131.68	−139.18	−135.42

[a] Calculated using eq 1, CSGT-B3LYP/6-311+G**//B3LYP/6-311+G**. [b] Calculated using eq 2, CSGT-B3LYP/6-311+G**//B3LYP/6-311+G**. [c] Calculated using eq 3, CSGT-B3LYP/6-311+G**//B3LYP/6-311+G**.

borane dianions, $B_nH_n^{2-}$, and *closo*-monocarbaborane anions, $CB_{n-1}H_n$. The plots of Λ vs cluster size confirm and emphasize our earlier conclusions for 5- to 12-vertex clusters (Figure 6 and Table 11): (a) the patterns of the Λ values of three sets of clusters are remarkably similar, and (b) the Λ's of all three sets tend to increase in magnitude with increasing cluster size from 5 to 12 vertexes, although individual deviations are apparent. The differences Λ between the *closo*-$CB_{n-1}H_n^-$ and *closo*-$B_nH_n^{2-}$ data sets are larger than those

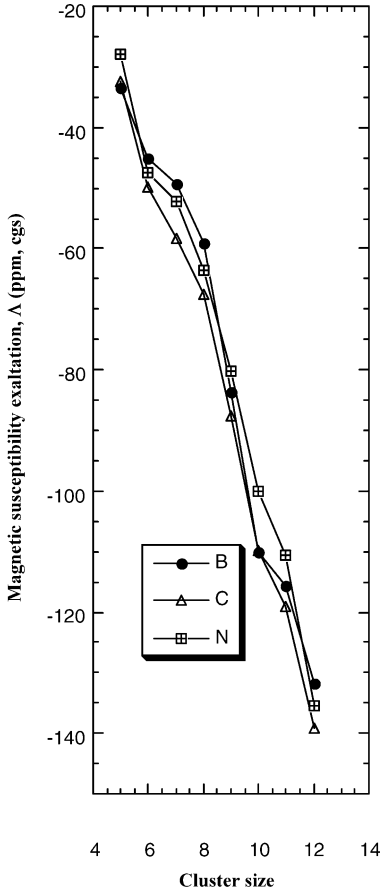

Figure 6. Plot of the magnetic susceptibility exaltations, Λ (ppm cgs, Table 11), of *closo*-borane dianions, $B_nH_n^{2-}$, and the most stable *closo*-monocarbaboranes $CB_{n-1}H_n^-$ and *closo*-azaboranes $NB_{n-1}H_n$ vs cluster size.

between the corresponding *closo*-$CB_{n-1}H_n^-$ and *closo*-$NB_{n-1}H_n$ sets.

The Relationships of NICS and the Magnetic Susceptibility, χ, with the Relative Stability of the Positional Isomers of *closo*-Azaboranes, $NB_{n-1}H_n$ ($n = 5-12$). We found earlier that the magnetic aromaticity ordering (based on NICS and magnetic susceptibilities) of the positional isomers of the *closo*-monocarborane anions, $CB_{n-1}H_n^-$ ($n = 5-12$), and of the *closo*-dicarboranes, $CB_{n-2}H_n$ ($n = 5-12$), did not always agree with the trend of the relative stabilities; other energy effects, such as topological charge stabilization and connectivity, can dominate.[30] Such discrepancies among aromaticity criteria can be even more pronounced with the *closo*-azaboranes, $NB_{n-1}H_n$ ($n = 5-12$), since the larger B−N electronegativity difference can result in considerable electron localization at nitrogen.

Negative NICS values (Table 13), ascribed to diatropic ring currents, characterize the degree of three-dimensional aromaticity of all the $NB_{n-1}H_n$ ($n = 5-12$) *closo*-azaboranes and their positional isomers directly. In contrast, the magnetic susceptibility χ depends on a higher power of the volume of a three-dimensional system and does not allow a simple comparison of *closo*-azaboranes of different sizes. However, χ is not very sensitive to the connectivity for systems with roughly the same volume. Hence, the relative aromaticity of the *closo*-azaboranes isomers can be deduced directly from the χ values (Table 13).

Table 12. Relative Energies of *closo*-Monocarbaborane Anions, $CB_{n-1}H_n^-$ ($n = 5-12$),[a] Nucleus Independent Chemical Shifts (NICS, ppm),[b] and Magnetic Susceptibilities (χ, ppm cgs)[c]

molecule	sym	rel energy[a]	NICS[b]	χ[c]
$CB_4H_5^-$				
1	C_{3v}	0.00	−17.42	−55.57
2	C_{2v}	23.31	−27.26	−63.61
$CB_5H_6^-$				
3	C_{4v}	0.00	−26.64	−71.47
$CB_6H_7^-$				
4	C_{2v}	0.00	−20.32	−78.42
5	C_{5v}	30.00	−20.24	−77.72
$CB_7H_8^-$				
6	C_s	0.00	−16.77	−86.18
7	C_s	22.10	−13.74	−83.23
8	C_{3v}	50.79	−19.79	−98.74
9	C_s	83.96	−18.16	−87.80
$CB_8H_9^-$				
10	C_{2v}	0.00	−20.15	−104.72
11	C_s	19.46	−20.77	−108.54
$CB_9H_{10}^-$				
12	C_{4v}	0.00	−24.85	−125.58
13	C_s	20.06	−28.20	−134.36
$CB_{10}H_{11}^-$				
14	C_s	0.00	−24.00	−133.14
15	C_s	18.20	−28.19	−140.56
16	C_s	19.88	−25.44	−136.13
17	C_2	30.90		
$CB_{11}H_{12}^-$				
18	C_{5v}	0.00	−28.00	−151.80
CBH_2^-	$C_{\infty v}$			−27.72

[a] From Table 2. [b,c] At CSGT-B3LYP/6-311+G**.

Table 13. Relative Energies of *closo*-Azaboranes, $NB_{n-1}H_n$ ($n = 5-12$),[a] Nucleus Independent Chemical Shifts (NICS, ppm),[b] and Magnetic Susceptibilities (χ, ppm cgs)[c]

molecule	sym	rel energy[a]	NICS[b]	χ[c]
NB_4H_5				
19	C_{3v}	0.00	−12.46	−42.52
20	C_2	14.18	+1.09	−22.41
20	C_s	48.28	−29.70	−53.87
20	C_{2v}	48.13	−29.69	−54.18
NB_5H_6				
21	C_{4v}	0.00	−25.88	−60.45
NB_6H_7				
22	C_s	0.00	−15.65	−63.61
23	C_{5v}	49.75	−18.88	−66.45
NB_7H_8				
24	C_s	0.00	−14.72	−73.65
25	C_{3v}	15.90	−20.21	−89.22
26	C_s	20.61	−2.01	−57.81
NB_8H_9				
27	C_s	0.00	−16.69	−88.68
27	C_{2v}	0.00	−16.61	−88.08
28	C_s	14.60	−15.31	−89.71
NB_9H_{10}				
29	C_{4v}	0.00	−19.96	−107.05
30	C_s	33.00	−26.57	−121.56
$NB_{10}H_{11}$				
31	C_s	0.00	−19.44	−115.96
32	C_s	32.61	−28.43	−129.91
33	C_s	36.48	−22.95	−121.97
34	C_s	40.42	−20.31	−120.13
$NB_{11}H_{12}$				
35	C_{5v}	0.00	−26.30	−139.35
NBH_2	C_v			−19.03

[a] From Table 3. [b,c] At CSGT-B3LYP/6-311+G**.

The relative aromaticites of the 11-vertex $NB_{10}H_{11}$ isomers, based on NICS and their χ values, do not agree with the ordering based on relative energies at all. The most stable isomer (2-$NB_{10}H_{11}$, **31**) is the least aromatic on the basis of the magnetic criteria (Table 13). Remarkable differences are found between the relative energy ordering of all the $NB_{10}H_{11}$ isomers, 2-$NB_{10}H_{11}$ (**31**) > 10-$NB_{10}H_{11}$ (**32**) > 8-$NB_{10}H_{11}$ (**33**) > 1-$NB_{10}H_{11}$ (**34**), and the magnetic property sequences, 10-$NB_{10}H_{11}$ (**32**) > 8-$NB_{10}H_{11}$ (**33**) > 1-$NB_{10}H_{11}$ (**34**) > 2-$NB_{10}H_{11}$ (**31**).

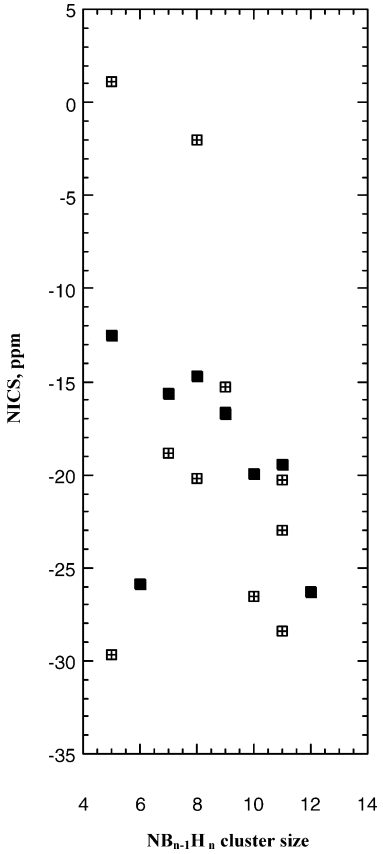

Figure 7. NICS computed at the center of all positional isomers of *closo*-azaboranes $NB_{n-1}H_n$ ($n = 5-12$) (in ppm, from Table 13) vs the cluster size. This figure points out that the most stable isomers often do not have the largest NICS values (shown by *n*; these points are plotted in Figures 4−6).

Aromaticity is associated with cyclic electron delocalization, which is most directly related to the magnetic criteria. However, thermodynamic stability is influenced by many additional factors including connectivity and charge stabilization. When substituted into borane clusters, electronegative heteroatoms such as carbon and especially nitrogen tend to localize the electrons; this may lead to decreased aromatictiy. When, however, such heteroatoms are placed at energetically unfavorable positions, the charge density tends to "smooth out" more, and a *greater* degree of delocalization (as detected by the magnetic criteria) results. We have observed this situation before.[34a,35]

In the 10-vertex cluster, the NICS and magnetic susceptibilities of 2-NB_9H_{10} (**30**), −26.57 and −121.56, respectively, are larger than those of 1-NB_9H_{10} (**29**) (NICS = −19.96 and χ = −107.05). This **30** > **29** order of the magnetic aromaticity data is opposite to the thermodynamic stability (**29** > **30**).

The stabilities of the 5-vertex isomers decrease in the sequence 1-NB_4H_5 (**19**, C_{3v}) > 2-NB_4H_5 (**20**, C_2) > 2-NB_4H_5

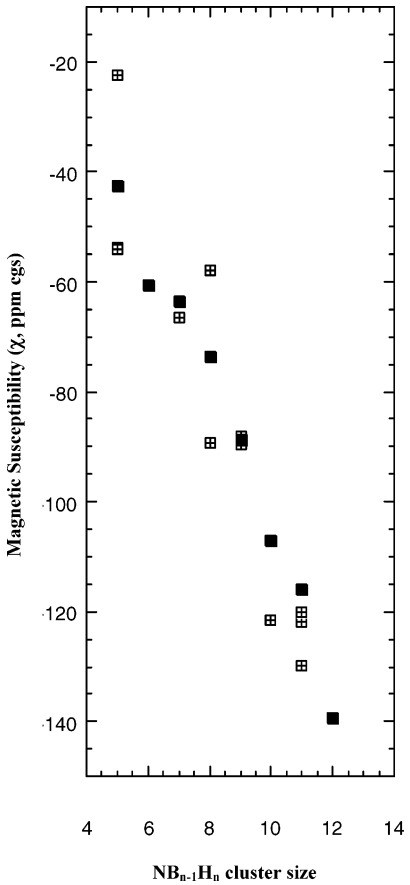

Figure 8. Magnetic susceptibilities χ computed for all positional isomers of *closo*-azaboranes $NB_{n-1}H_n$ ($n = 5-12$) (ppm cgs, from Table 13) vs the cluster size. This figure points out that the most stable isomers often do not have the largest NICS values (shown by *n*; these points are plotted in Figures 4−6).

(**20**, C_s) > 2-NB_4H_5 (**20**, C_{2v}) (Table 13). However, the order for both the NICS and the magnetic susceptibility is opposite: 2-NB_4H_5 (**20**, C_{2v}) > 2-NB_4H_5 (**20**, C_s) > 1-NB_4H_5 (**19**, C_{3v}) > 2-NB_4H_5 (**20**, C_2). This is another example where thermodynamic stability and aromaticity are not directly related in positional isomers.[34a,35] A similar situation, where the magnetic property order increases with decreasing thermodynamic stability, is found in 7-vertex species. The less stable 1-NB_6H_7 (**23**) has a larger NICS and a larger χ value than the 2-NB_6H_7 (**22**) isomer (Table 13).

In contrast, 9-vertex isomers do exhibit a direct correlation between the NICS aromaticity and stability trends: 4-NB_8H_9 (**27**, C_s) > 4-NB_8H_9 (**27**, C_{2v}) > 1-NB_8H_9 (**28**, C_s) (Table 13). The most stable NB_8H_9 positional isomer is the most aromatic on this basis. However, the magnetic susceptibilities of all positional isomers are nearly the same.

Conclusions

The relative energies of all the positional isomers of the *closo*-azaboranes, $NB_{n-1}H_n$, agree with topological charge stabilization considerations as well as with the Williams connectivity and the Jemmis−Schleyer six interstitial electron rules. The stabilities of the lowest energy positional isomers of *closo*-azaboranes, $NB_{n-1}H_n$, are like those of the isoelectronic, *closo*-borane dianions, $B_nH_n^{2-}$ ($n = 5-12$), and *closo*-monocarbaborane anions, $CB_{n-1}H_n^-$ ($n = 5-12$). The most symmetrical 6- and 12-vertex *closo* species, $B_{12}H_{12}^{2-}$ and $B_6H_6^{2-}$, $CB_{11}H_{12}^-$ and $CB_5H_6^-$, and $NB_{11}H_{12}$ and NB_5H_6, define the lines for each family shown in Figure 4. Each line serves as the basis for the quantitative comparison of the other members of each set. The reaction energies, ΔH, for all three sets of clusters tend to increase with increasing cluster size from 5 to 12 vertexes. The deviations of individual species (apparent in Figure 4) show quite similar trends but decrease from *closo*-$B_nH_n^{2-}$ to *closo*-$CB_{n-1}H_n^-$ and from *closo*-$CB_{n-1}H_n^-$ to *closo*-$NB_{n-1}H_n$.

The reaction energies, ΔH, in *closo*-$B_nH_n^{2-}$ are about twice as large as in *closo*-$CB_{n-1}H_n^-$; the same is true for *closo*-$CB_{n-1}H_n^-$ vs *closo*-$NB_{n-1}H_n$. These differences are due to the greater degree of electron localization at the more electronegative atom, carbon in the first comparison and nitrogen in the second. Hence, the replacement of boron by the much more electronegative nitrogen in the *closo*-$NB_{n-1}H_n$ family leads to the largest leveling effect.

The magnetic criteria, NICS values, and magnetic susceptibilities document the three-dimensional aromaticity in *closo*-$NB_{n-1}H_n$. NICS of the $B_nH_n^{2-}$, $CB_{n-1}H_n^-$, and $NB_{n-1}H_n$ *closo* sets show remarkably similar patterns vs the cluster size. The $B_nH_n^{2-}$ NICS values tend to be the largest among the three sets but not in all cases. The 6- and 12-vertex species are more aromatic than the other members of their families (Figure 6). The most stable isomers with a given composition need not be the most aromatic (as based on the magnetic criteria), since the overall bonding energies may depend on other factors such as connectivity and topological charge stabilization. Electronegative atoms, such as nitrogen, substituted into borane cages tend to localize the electrons and decrease the aromaticity.

Acknowledgment. This work was supported by the University of Georgia, by National Science Foundation Grant CHE-0209857, and by the Natural Sciences and Engineering Research Council of Canada and the Canada Council for the Arts (Killam Fellowship to T.T.T.).

IC0340783